12-1973

Kinetics of the Metal Exchange Reaction between N, N'-BIS (2-Picolyl) Ethylenediaminenickel (II) and Copper (II)

Craig Lee Barsuhn

KINETICS OF THE METAL EXCHANGE REACTION BETWEEN N,N'-BIS(2-PICOLYL)ETHYLENEDIAMINENICKEL(II) AND COPPER(II)

by

Craig Lee Barsuhn

A Thesis
Submitted to the
Faculty of The Graduate College
in partial fulfillment
of the
Degree of Master of Arts

Western Michigan University
Kalamazoo, Michigan
December, 1973

ACKNOWLEDGEMENTS

The author wishes to express sincere appreciation to Dr. Ralph K. Steinhaus for timely suggestions and constructive criticism in the course of this study. Thanks are also given to the faculty of the Department of Chemistry at Western Michigan University and especially to the members of the author's committee, Dr. James A. Howell and Dr. Robert H. Anderson. The financial support provided by the University is greatly appreciated.

The author also expresses sincere gratitude to his family for constant encouragement and understanding during his graduate study.

Craig Lee Barsuhn

MASTERS THESIS M-5083

BARSUHN, Craig Lee
KINETICS OF THE METAL EXCHANGE REACTION BETWEN N,N'-BIS(2-PICOLYL)ETHYLENEDIAMINE-NICKEL(II) AND COPPER(II).

Western Michigan University, M.A., 1973
Chemistry, inorganic

TABLE OF CONTENTS

	Page
ACKNOWLEDGEMENTS	ii
LIST OF TABLES	iv
LIST OF FIGURES	vi
INTRODUCTION	1
APPARATUS AND REAGENTS	4
Apparatus	4
Reagents	4
EXPERIMENTAL	10
Spectrophotometric Study of Reactants and Products	10
Standardization of $NiBPEDA^{+2}$ Solution	10
Kinetics of the Reaction of Cu^{+2} with $NiBPEDA^{+2}$	15
Determination of Ni^{+2} Stability Constants of AEAMP	27
RESULTS AND DISCUSSION	30
Resolution of the Rate Data	30
Mechanism of the Exchange Reaction	46
APPENDIX	63
BIBLIOGRAPHY	65

LIST OF TABLES

TABLE NO.		Page
1	Molar Absorptivity of Copper(II) as a Function of pH	11
2	Values Necessary to Calculate $[Ni^{+2}]$ and [BPEDA] by the Secondary Method	13
3	Concentrations of Ni^{+2} and BPEDA Calculated by the Secondary Method	14
4	Experimental Conditions for Reaction Rate Studies .	16
5	Comparison of Exchange Rate Calculated by the Initial Rates Method to Values Obtained by Measurement of A_∞ and Plotting of the Integrated Rate Equation	19
6	Kinetic Data for the Exchange Reactions	20
7	Experimental Data for the Potentiometric Titration of AEAMP-Ni^{+2} with NaOH	28
8	Acid Dissociation Constants and Ni^{+2} Stability Constants for AEAMP	29
9	Stability Constants and Formation Rate Constants for Individual Species of the $NiBPEDA^{+2}$ System .	32
10	Comparison of Possible Dinuclear Intermediates for the Exchange of $NiBPEDA^{+2}$ with Cu^{+2} to Known Systems	49

LIST OF TABLES (Cont.)

TABLE NO.		Page
11	Stability Constants and Rate Constants Used in Making Comparisons Shown in Table 10	52
12	Comparison of Stability Constants Between Aliphatic and Aromatic Nitrogen Complexes with Nickel(II) and Copper(II)	54
13	Effect of Hydroxide on Stability of Copper(II) Complexes	59
14	Comparison of Rate Constants for the Attack of Cu^{+2} and $CuOH^{+}$ on Various Complexes	61

LIST OF FIGURES

FIGURE NO.		Page
1	pH dependence of the rate of the exchange reaction	33
2	Distribution of copper species as a function of pH	37
3	Initial resolution of rate constant $k^{NiL}_{Cu^{+2}}$	38
4	Resolution of rate constant $k^{NiL}_{Cu_2(OH)_2^{+2}}$	39
5	Non-linear plot demonstrating that $CuOH^+$ and $Cu_2(OH)_2^{+2}$ are individual species	41
6	Comparison of the theoretical curve to experimentally determined values of k_o-k_d at total copper concentration = 4.404×10^{-3} M	43
7	Comparison of the theoretical curve to experimentally determined values of k_o-k_d at total copper concentration = 8.315×10^{-3} M	44
8	Comparison of the theoretical curve to experimentally determined values of k_o-k_d at total copper concentration = 1.743×10^{-2} M	45
9	Mechanism for the reaction of Cu^{+2} with $NiBPEDA^{+2}$.	55

INTRODUCTION

Metal exchange reactions of multidentate ligand complexes, represented by equation 1, have been the subject of very extensive study (1-6).

$$M + M'L \rightleftharpoons ML + M' \qquad (1)$$

Systematic studies involving comparisons between a series of similar ligands and a series of similar metals has been very fruitful in revealing the mechanism by which these reactions proceed and in forming a basis from which mechanisms and rate constants can accurately be predicted.

Detailed studies have shown the mechanism of these reactions to be the successive breaking of a series of coordinate bonds from the metal-ligand complex, followed by a stepwise coordination to the attacking metal (3). This process leads to the formation of a dinuclear intermediate found in all cases where sterically possible (5), followed by breakup to form products. Depending upon the system, the position of the rate-determining step has been found to be a function of pH (6-8), attacking metal concentration (7,8), relative stability of the intermediate metal segments (3) and the relative rate of water loss of the metals involved (9). In most cases the ratio of rate constants of the system can be approximated by the ratio of relative stability constants for the dinuclear intermediates involved (3).

Other investigations have dealt with the kinetic effect ions coordinated to the attacking metal have upon the exchange rate. Hydroxide appears to significantly accelerate the exchange rate in all cases where azide and acetate have relatively small effects.

Most of the systems studied thus far have involved aminocarboxylate ligands, whereas only two reports of metal exchange reactions involving polyamine ligands have appeared (10, 11). None of these have dealt with the interesting class of polyamines having both aliphatic and aromatic dentate sites. These ligands are unusual in that the aromatic nitrogens are relatively quite acidic yet without a corresponding decrease in metal stability. Thus their complexes are far more stable in acidic solutions than the complexes of the aliphatic analogues.

The present study is concerned with the metal exchange reaction between N,N'-bis(2-picolyl)ethylenediaminenickel(II) ($NiBPEDA^{+2}$) and copper(II). BPEDA (structure I) has both aromatic and aliphatic nitrogens positioned such that three five membered chelate rings can form with a metal ion.

I

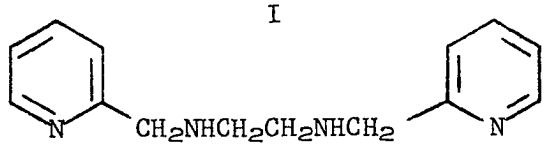

II

$H_2NCH_2CH_2NHCH_2CH_2NHCH_2CH_2NH_2$

The rate of the exchange reaction is shown to increase with increasing pH in the region where hydrolysis of copper ion is significant. The increase in rate is explained as $CuOH^{+}$ and $Cu_2(OH)_2^{+2}$ being more reactive than Cu^{+2} towards $NiBPEDA^{+2}$.

A general mechanism is proposed for the exchange reaction and is found to be consistent with the kinetic data. The dinuclear intermediate prior to the rate-determining step is characterized as being two nitrogens, an amionmethylpyridine (AMP) unit, bonded to nickel and an aliphatic nitrogen bonded to copper with the terminal pyridine nitrogen unbonded.

Comparison to other systems points out interesting differences in the reaction mechanism due to the influence of the ligand.

APPARATUS AND REAGENTS

Apparatus

All absorbance measurements and recordings were made with a Cary Model 14 Spectrophotometer using a hydrogen or tungsten source where appropriate, slit control 20, dynode voltage setting 2, and a 10 mm or 100 mm quartz cell in a water jacketed cell holder.

All pH measurements were made with a Beckman Research Model 1019 pH meter. A glass-calomel electrode pair was used. In order to prevent interference due to potassium perchlorate precipitation, a saturated sodium chloride solution was substituted for potassium chloride in the calomel electrode.

During kinetic measurements all solutions were maintained at 25 $\pm$ 0.1° C with a circulating constant temperature bath.

Reagents

All solutions were made using deionized water prepared by passing distilled water through a column of Amberlite MB-3 mixed bed resin. All chemicals were reagent grade unless otherwise specified.

Primary Standard Copper Nitrate

Reagent grade copper wire (B & A) was cleaned with dilute nitric acid, rinsed with water, dried, weighed and dissolved in a minimum amount of nitric acid. After dilution to volume the concentration was 0.09937 M.

Ethylenediaminetetraacetic Acid (EDTA)

Disodium(ethylenedinitrilo)tetraacetate dihydrate (J. T. Baker) was dissolved in water. The solution was standardized against standard copper nitrate solution at pH 10 using murexide as the indicator and a pH 10 buffer. (12)

Copper Perchlorate

Copper perchlorate hexahydrate (J. T. Baker) was dissolved in water. The resulting solution was standardized against standard EDTA using murexide indicator and a pH 10 ammoniacal buffer. (12)

Nickel Chloride

Nickel chloride hexahydrate (J. T. Baker) was dissolved in water. The solution was standardized against standard EDTA solution at pH 10 using murexide indicator and a pH 10 ammoniacal buffer. (12)

Ammoniacal Buffer, pH 10

To an aqueous solution of 70 grams of ammonium chloride was added 570 ml concentrated ammonium hydroxide solution. After dilution to 1 liter the solution was approximately pH 10.

N,N'-bis(2-picolyl)ethylenediamine (BPEDA)

N,N'-bis(2-picolyl)ethylenediimine was prepared as summarized by the following reaction.

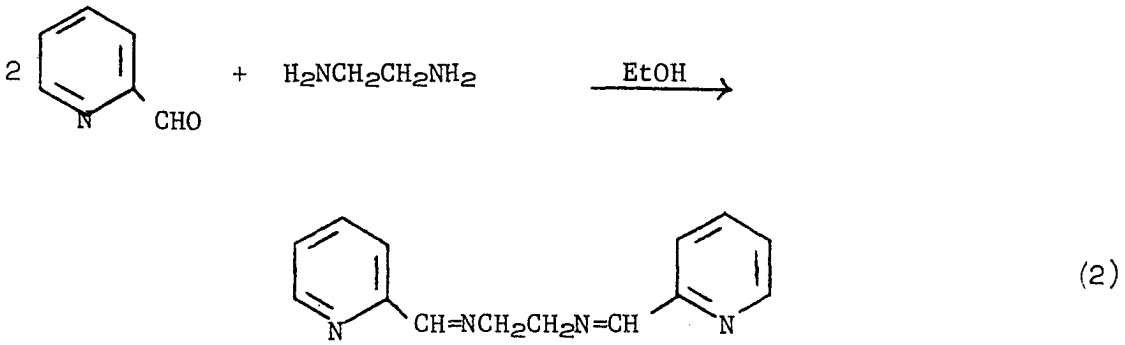

(2)

Thirty grams (0.28 mole) of pyridine-2-aldehyde (Aldrich) was dissolved in approximately 50 ml of absolute ethanol in a 300 ml round bottom flask. To this solution was added 8.4 grams (0.14 mole) of ethylenediamine with rapid stirring. After standing for about 30 minutes the solvent was removed using a rotary evaporator at about 60° C. As the solvent was removed the product solidified into a tan wax-like solid, which yielded pale yellow crystals upon recrystallization from low-boiling (30-60°) petroleum ether. The recrystallized product melted at 66-67°C compared to the literature value of 67-68° C. (13)

N,N'-bis(2-picolyl)ethylenediamine was prepared from the imine as shown in the following reaction.

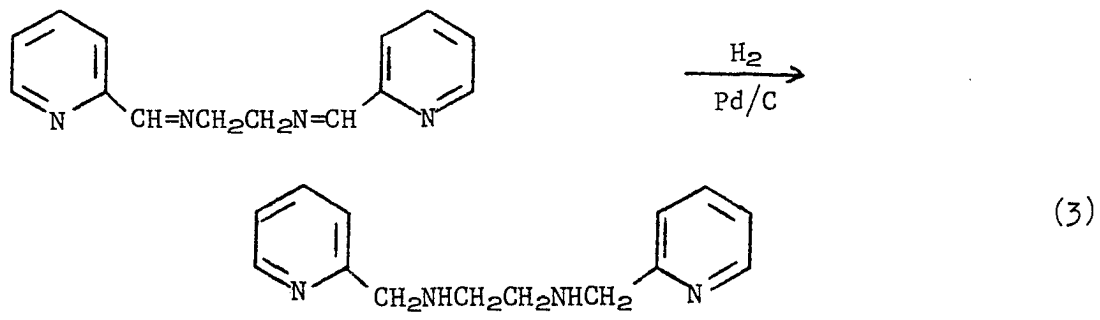

(3)

Thirty grams (0.13 mole of N,N'-bis(2-picolyl)ethylendiimine dissolved in ethanol containing 1.5 grams of 10% Pd/C catalyst was reduced for 4 to 5 hours in a Parr hydrogenation apparatus with a hydrogen pressure of 50 p.s.i. at room temperature. The solution was filtered to remove the catalyst and the solvent removed using a rotary evaporator at about 60° C. The product, an extremely viscous, yellow liquid, was diluted with anhydrous ethyl ether. Dry HCl was passed through this solution to precipitate the desired product as the tetrahydrochloride. Double recrystallization from methanol-ether (4:1) yielded colorless crystalline material which melted with decomposition at 223° C as reported by Gruenwedel (14).

Analysis for $C_{14}H_{22}N_4Cl_4$

	%C	%H	%N
Calculated	43.32	5.71	14.44
Found	42.21	5.65	14.12

The tetrahydrochloride was dissolved in water and standardized against copper nitrate using the mole ratio method. Several restandardizations of the stock solution over a period of a week showed it to be unstable under ordinary conditions and the compound was thereafter stored in crystalline form until needed.

NiBPEDA Solution

The tetrahydrochloride of BPEDA was dissolved in water containing a 5% mole excess of nickel chloride. The solution was adjusted to approximately pH 10 by the addition of concentrated aqueous sodium

hydroxide. The excess nickel was removed as the precipitated hydroxide by drawing the solution through a Millipore 0.45 micron filter. The pH of the filtered solution was immediately adjusted to pH 5 by the addition of concentrated perchloric acid.

CuBPEDA Solution

CuBPEDA was prepared in a manner similar to NiBPEDA using copper perchlorate.

2-Pyridylmethyl-2'-aminoethylamine (Aminoethylaminomethylpyridine: AEAMP)

AEAMP was prepared as shown in reaction 4 (15).

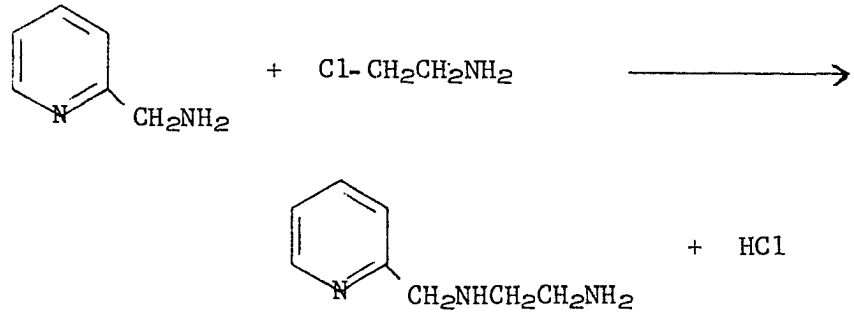

(4)

A 13.65 gram (0.17 mole) sample of 2-chloroethylamine monohydrochloride (Aldrich) was neutralized with saturated aqueous potassium carbonate. After removal of the precipitated KCl, the free base solution was added dropwise with rapid stirring to a refluxing solution of 25 grams (0.27 mole) of 2-aminomethylpyridine (Aldrich) dissolved in an equal volume of ethanol. The mixture was refluxed for 2 hours after all the 2-chloroethylamine had been added. The ethanol

was removed by rotary evaporation, the residue poured onto crushed ice and the mixture neutralized with 25% KOH followed by the addition of excess KOH pellets. The dark orange-brown solution was extracted several times with chloroform, the chloroform extracts combined and dried over anhydrous $MgSO_4$. After removal of the chloroform by rotary evaporation the residue was vacuum distilled. The liquid boiling at 120° C at 0.5 mm Hg was collected. After a second distillation the liquid was dissolved in ethanol and the trihydrochloride was precipitated by saturating the solution with dry HCl. Recrystallization from methanol-ether (4:1) produced a fine white crystalline material which melted at 209° C compared with a literature value of 217° C. (15) Analysis for $C_8H_{16}N_3Cl_3$.

	%C	%H	%N
Calculated	36.87	6.19	16.12
Found	36.99	6.17	16.42

The trihydrochloride was dissolved in water and standardized potentiometrically against standard carbonate-free sodium hydroxide solution.

EXPERIMENTAL

Spectrophotometric Study of Reactants and Products

The spectra of all reactants and products of equation 5 were obtained from 200 to 800 nm.

$$NiBPEDA^{+2} + Cu^{+2} \rightleftharpoons CuBPEDA^{+2} + Ni^{+2} \qquad (5)$$

Maxima were observed for $CuBPEDA^{+2}$ and $NiBPEDA^{+2}$ at 610 nm and 560 nm, respectively. The maximum change in absorbance from reactants to products was seen at 610 nm and this wavelength was used for all kinetic studies. The molar absorptivities of Ni^{+2}, $NiBPEDA^{+2}$ and $CuBPEDA^{+2}$ at 610 nm were 0.1, 4.167, and 154.1, respectively, at 25 $\pm$ 0.1° C. and 0.1 M ionic strength. The molar absorptivity of Cu^{+2} varied with pH. Molar absorptivity as a function of pH is listed in Table 1.

Standardization of $NiBPEDA^{+2}$ Solution

The concentration of $NiBPEDA^{+2}$ was determined by measuring the nickel content of $NiBPEDA^{+2}$ in the following manner: A 2 ml aliquot of approximately 0.05 M $NiBPEDA^{+2}$ was transferred to a 100 ml volumetric flask, 10 ml pH 10 buffer and 40 ml of 1M NaCN (100-fold excess) were added and diluted to volume. From 1 to 5 ml aliquots of this solution were diluted to 100 ml with water and the absorbance measured at 268 nm. The absorbance at this wavelength and pH is due to $Ni(CN)_4^{=}$ and BPEDA, which have molar absorptivities of 1.176×10^4 and 4.74×10^3, respectively, and is represented mathematically as

TABLE 1

MOLAR ABSORPTIVITY OF COPPER(II) AS A FUNCTION OF pH.

$[Cu(ClO_4)_2]$ = 2.491 x 10^{-2} M Temp. = 25 ± .1° C.

Cell pathlength = 10.0 cm Wavelength = 610 nm

pH	Absorbance	Molar Absorptivity
3.93	0.274	1.10
4.64	0.280	1.12
4.90	0.286	1.14
5.13	0.304	1.22
5.24	0.317	1.27
5.41	0.372	1.49

$$A = \epsilon_{(Ni(CN)_4^{=})}[Ni(CN)_4^{=}]b + \epsilon_{BPEDA}[BPEDA]b \quad (6)$$

where A is the absorbance, ϵ is the molar absorptivity of the subscripted species, b is the cell path length in cm and [ ] represents molar concentration of the enclosed species. Since

$$[Ni(CN)_4^{=}] = [BPEDA] = C \quad (7)$$

then

$$C = A/(\epsilon_{(Ni(CN)_4^{=})} + \epsilon_{BPEDA})b \quad (8)$$

The validity of the above standardization procedure was confirmed by determining the concentration of both Ni^{+2} and BPEDA using a different method. An aqueous solution of the tetrahydrochloride of BPEDA was prepared and standardized against standard copper perchlorate solution spectrophotometrically by the mole ratio method. This standardized solution was used immediately to determine the molar absorptivity of BPEDA at four different wavelengths. A solution of $Ni(CN)_4^{=}$ of known concentration was prepared from standard $NiCl_2$ and excess NaCN and the molar absorptivity of $Ni(CN)_4^{=}$) was determined at these same wavelengths. The absorbance of a $NiBPEDA^{+2}$ solution containing a 100 fold excess of CN^{-} was then determined at each of the four wavelengths. The concentration of both Ni^{+2} and BPEDA was obtained by simultaneous solution of several pairs of the following equation.

$$\epsilon_{(Ni(CN)_4^{=})}[Ni(CN)_4^{=}]b + \epsilon_{BPEDA}[BPEDA]b = A \quad (9)$$

Data and results of this method are summarized in Tables 2 and 3.

TABLE 2

VALUES NECESSARY TO CALCULATE $[Ni^{+2}]$ AND [BPEDA] BY THE SECONDARY METHOD.

$[BPEDA] = 1.392 \times 10^{-4}\underline{M}$, $[Ni(CN)_4^{=}] = 7.976 \times 10^{-5}\underline{M}$, $[NiBPEDA^{+2}] = 5.32 \times 10^{-5}\underline{M}$

Wavelength (nm)	$A_{Ni(CN)_4^{=}}$	$\epsilon_{Ni(CN)_4^{=}}$	A_{BPEDA}	ϵ_{BPEDA}	$A_{NiBPEDA^{+2}}$
250	0.075	9.40×10^2	0.699	4.81×10^3	0.303
261	0.478	5.99×10^3	1.038	7.38×10^3	0.713
268	0.955	1.20×10^4	0.694	4.98×10^3	0.304
290	0.199	2.50×10^3	0.004	2.87×10^1	0.128

TABLE 3

CONCENTRATIONS OF Ni^{+2} AND BPEDA CALCULATED BY THE SECONDARY METHOD.

Wavelengths Used (nm)	$[Ni^{+2}]$, M	[BPEDA], M
250 & 261	5.47×10^{-5}	5.23×10^{-5}
261 & 268	5.35×10^{-5}	5.32×10^{-5}
268 & 290	5.06×10^{-5}	5.98×10^{-5}

Kinetics of the Reaction of Cu^{+2} with $NiBPEDA^{+2}$

The kinetics of the reaction of Cu^{+2} with $NiBPEDA^{+2}$ were studied by following the increase in absorbance at 610 nm due to the formation of $CuBPEDA^{+2}$. The reaction was followed under pseudo-first order conditions by maintaining a Cu^{+2} concentration of at least 10-fold molar excess. The experimental conditions are summarized in Table 4.

The solutions for the kinetic studies were prepared in the following manner: Solutions of copper perchlorate of the required concentration were prepared by dilution of appropriate volumes of stock $Cu(ClO_4)_2$ containing sodium perchlorate for ionic strength control. The pH was adjusted by addition of concentrated solutions of NaOH or $HClO_4$. $NiBPEDA^{+2}$ solutions were prepared by diluting appropriate volumes of stock $NiBPEDA^{+2}$. These solutions were placed in a water bath maintained at 25 $\pm$ 0.1 C for at least thirty minutes before use.

The spectrophotometer was allowed to warm up for 15 minutes before use. Zero absorbance was set using water filled cells. A water filled cell was always used as the reference cell.

Aliquots of both the $NiBPEDA^{+2}$ and $Cu(ClO_4)_2$ solutions were pipetted into a flask and mixed well by shaking. The spectrophotometer cell was rinsed several times with a portion of this solution before finally being filled. The cell was placed in a thermostated water jacket in the spectrophotometer and the absorbance recording begun exactly one minute after mixing. Initially, recordings were made continuously for the first 100 minutes and then at appropriate intervals for 4 to 5 half-lives. A_∞ was measured when the absorbance was at a final

TABLE 4

EXPERIMENTAL CONDITIONS FOR REACTION RATE STUDIES

$[NiBPEDA^{+2}]$	4.05×10^{-4} to 8.10×10^{-4} M
$[Cu^{+2}]$	4.404×10^{-3} to 1.743×10^{-2} M
Ionic strength	0.1 M
pH range	3.44 - 6.07
Temperature	25± 0.1° C.
Wavelength	610 nm
Slit program	20
Light source	Tungsten filament lamp
Cell pathlength	100 nm

maximum. In later studies the absorbance was measured for the first 200 minutes only.

The pH of the solution was determined soon after mixing and was found to remain constant through the reaction. The pH range over which kinetic measurements could be made was limited at higher pH by the formation of a copper hydroxide precipitate and at lower pH by the extreme sluggishness of the exchange reaction.

The rate expression for reaction 1 may be expressed by the following second-order equation,

$$\frac{-d[NiBPEDA^{+2}]}{dt} = \frac{d[CuBPEDA^{+2}]}{dt} = k[NiBPEDA^{+2}][Cu_T] \qquad (10)$$

where Cu_T refers to the sum of individual copper species present.

Assuming a constant copper concentration due to a 10-fold or greater excess equation 10 reduces to the pseudo-first-order equation,

$$\frac{-d[NiBPEDA^{+2}]}{dt} = \frac{d[CuBPEDA^{+2}]}{dt} = k_o[NiBPEDA^{+2}] \qquad (11)$$

where k_o is the observed first order rate constant

$$k_o = k[Cu_T] \qquad (12)$$

Integration of equation 11 yields

$$Ln[NiBPEDA^{+2}] = Ln[NiBPEDA^{+2}]_o - k_o t \qquad (13)$$

where $[NiBPEDA^{+2}]_o$ is the initial concentration. The loss of $NiBPEDA^{+2}$ is equal to the formation of $CuBPEDA^{+2}$ and is related to change in absorbance as the reaction progresses. Equation 14 relates the final ab-

sorbance, A_∞; the absorbance at any time t, A_t, the molar absorptivities of reactants and products and the cell path length to the concentration of $NiBPEDA^{+2}$ and is derived in the appendix.

$$[NiBPEDA^{+2}] = \frac{A_\infty - A_t}{b(\epsilon_{CuBPEDA^{+2}} - \epsilon_{NiBPEDA^{+2}} - \epsilon_{Ni^{+2}} - \epsilon_{Cu^{+2}})} \quad (14)$$

Plots of log $(A_\infty - A_t)$ versus time showed excellent linear behavior demonstrating first-order dependence on $NiBPEDA^{+2}$.

Due to the impracticability of determining A_∞ for each reaction because of the time involved, the method of initial rates was used in determining k_o after the kinetic behavior of the system had been well established. To employ this method the assumption must be made that over a small enough time interval $-\Delta NiBPEDA^{+2}/\Delta t$ is constant. With the use of a digital computer k_o could be determined over many small overlapping time intervals from a knowledge of A, t, initial concentration and molar absorptivities. By taking the average of these many individual values, k_o could be determined by following only the first 200 minutes of a reaction which could take up to 14 days to reach equilibrium. Values obtained by this method were checked with those obtained by measurement of A_∞ and subsequent plotting of the integrated rate equation using the same solutions. The results, which gave excellent agreement, are shown in Table 5. Table 6 lists the values of k_o as a function of pH and total copper concentration.

TABLE 5

COMPARISON OF EXCHANGE RATE CALCULATED BY THE INITIAL RATES METHOD TO VALUES OBTAINED BY MEASUREMENT OF A_∞ AND PLOTTING OF THE INTEGRATED RATE EQUATION.

$[NiBPEDA^{+2}] = 8.10 \times 10^{-4}$ M $[Cu^{+2}] = 7.49 \times 10^{-3}$ M

$\mu = 0.1$ M T = 25 ± 0.1° C

pH	Rate by Plotting (sec^{-1})	Rate by Initial Rates (sec^{-1})
4.33	5.16×10^{-6}	5.30×10^{-6}
4.34	5.05×10^{-6}	5.16×10^{-6}
4.36	5.08×10^{-6}	5.22×10^{-6}
5.08	7.84×10^{-6}	8.35×10^{-6}
5.09	8.14×10^{-6}	8.35×10^{-6}
5.10	8.04×10^{-6}	8.51×10^{-6}
5.58	1.82×10^{-5}	2.28×10^{-5}
5.61	2.26×10^{-5}	2.57×10^{-5}
5.62	2.18×10^{-5}	2.31×10^{-5}

TABLE 6

KINETIC DATA FOR THE EXCHANGE REACTIONS.

pH	$k_o \times 10^5$, sec^{-1}
	$Cu_T = 4.404 \times 10^{-3}$ M
3.73	0.224
4.01	0.272
4.09	0.228
4.21	0.269
4.30	0.294
4.31	0.303
4.32	0.268
4.33	0.279
4.39	0.282
4.48	0.314
4.54	0.308
4.68	0.335
4.69	0.334
4.99	0.421
5.25	0.715
5.28	0.708
5.50	1.12
5.52	1.12
5.55	1.20

TABLE 6 (Cont.)

5.59	1.56
5.61	1.56
5.65	1.71
5.70	2.10
5.80	2.60
5.89	3.17
5.97	4.21
6.01	3.96
6.02	4.41
6.03	3.95
6.07	4.79

$Cu_T = 7.471 \times 10^{-3} M$

5.00	0.528
5.00	0.540
5.00	0.559
5.32	1.10
5.33	1.08
5.33	1.10
5.62	2.42
5.62	2.46
5.63	2.43

TABLE 6 (Cont.)

$Cu_T = 7.948 \times 10^{-3}$ M	
3.96	0.385
4.43	0.495
4.66	0.520
5.04	0.709
5.23	1.03
5.39	1.37
$Cu_T = 8.315 \times 10^{-3}$ M	
3.42	0.277
3.44	0.274
3.44	0.324
3.69	0.260
3.69	0.277
3.71	0.268
3.97	0.305
3.98	0.318
4.30	0.378
4.32	0.340
4.33	0.315
4.64	0.460
4.68	0.466
5.08	0.479
5.08	0.541
5.08	0.581

TABLE 6 (Cont.)

5.30	0.541
5.31	0.597
5.32	0.617
5.40	1.50
5.54	2.11
5.61	2.74

$Cu_T = 9.962 \times 10^{-3}$ M

4.96	0.681
4.96	0.696
4.99	0.719
5.04	0.773
5.04	0.775
5.04	0.815
5.15	1.01
5.31	1.33
5.31	1.39
5.31	1.35
5.33	1.40
5.33	1.42
5.33	1.57
5.44	1.95
5.44	1.99
5.49	1.94
5.58	2.88

TABLE 6 (Cont.)

5.59	2.83
5.60	2.90
5.60	3.45
5.60	3.42
5.60	3.46

$Cu_T = 1.245 \times 10^{-2}$ M

4.61	0.554
4.65	0.535
4.65	0.569
5.01	0.865
5.04	0.777
5.04	0.819
5.31	1.43
5.31	1.49
5.32	1.50
5.48	2.19
5.49	2.11
5.49	2.12
5.65	3.82
5.65	3.90
5.67	3.71

TABLE 6 (Cont)

	$Cu_T = 1.495 \times 10^{-2}$ M
4.32	0.489
4.32	0.512
4.33	0.491
4.49	0.523
4.50	0.522
4.59	0.514
4.59	0.548
4.59	0.563
4.84	0.734
4.84	0.743
4.87	0.807
5.05	1.04
5.05	1.07
5.06	1.26
5.17	1.30
5.18	1.38
5.20	1.43
5.32	1.78
5.33	1.72
5.33	1.74
5.43	2.12
5.43	2.26
5.44	2.11

TABLE 6 (Cont.)

5.55	4.02
5.55	4.02
$Cu_T = 1.743 \times 10^{-2}$ M	
4.27	0.668
4.28	0.643
4.30	0.620
4.97	1.00
4.97	1.00
4.97	1.07
5.25	1.64
5.25	1.70
5.25	1.75
5.56	3.81
5.58	3.86
5.58	3.91

Determination of Ni^{+2} Stability Constants of AEAMP

The complex stability constants of Ni^{+2} with AEAMP, described by equations 15 and 16, were obtained using

$$K_1 = \frac{[NiAEAMP^{+2}]}{[Ni^{+2}][AEAMP]} \qquad (15)$$

$$K_2 = \frac{[(Ni)_2AEAMP^{+4}]}{[Ni^{+2}][NiAEAMP^{+2}]} \qquad (16)$$

the method of Bjerrum (16) described by Jonassen, LeBlanc and Rogan (17). Data from potentiometric titrations were obtained as follows. A 100 ml aliquot of a solution which was 1.007×10^{-3} M in respect to AEAMP·3HCl, 0.1 M in $NaClO_4$, and 5.37×10^{-4} M in $Ni(ClO_4)_2$ was delivered into a four-necked flask immersed in a constant temperature bath maintained at 25 ± 0.1° C. The four-necked flask was equipped with a mechanical stirrer, a glass and calomel electrode pair and a nitrogen bubbler. The titration was carried out by the addition of 0.1727 N carbonate-free NaOH from a 5 ml buret. The results are listed in Table 7. The values of log K_1 and log K_2 were calculated using the acid dissociation constants determined by Romary, Barger and Zachariasen (15) and are listed in Table 8.

TABLE 7

EXPERIMENTAL DATA FOR THE POTENTIOMETRIC TITRATION OF AEAMP-Ni^{+2} WITH NaOH.

[NaOH] = 0.1727 N Initial volume = 100.0 ml

μ = 0.1 M $[AEAMP \cdot 3HCl]_i = 1.007 \times 10^{-3}$ M

T = 25 ± 0.1° C $[Ni(ClO_4)_2 = 5.370 \times 10^{-4}$ M

NaOH (ml)	pH
0.000	2.898
0.100	2.955
0.298	3.091
0.401	3.181
0.500	3.257
0.597	3.319
0.694	3.408
0.800	3.521
0.896	3.635
1.002	3.780
1.131	3.992
1.220	4.151
1.301	4.285
1.403	4.474
1.500	4.675
1.600	4.954
1.707	5.667
1.740	7.020
1.820	7.720
2.011	8.032
2.270	8.851
2.392	9.195

TABLE 8

ACID DISSOCIATION CONSTANTS AND Ni^{+2} Stability CONSTANTS FOR AEAMP

Constant	Value	Reference
pK_1 [a]	1.84	15
pK_2	5.91	15
pK_3	9.54	15
Log K_1 [b]	11.90	This work
Log K_2	9.76	This work

[a] $pK_1 = pH - \text{Log} \frac{[AH_{n-1}]}{[AH_n]}$

[b] $K_1 = \frac{[ML]}{[M][L]}$

RESULTS AND DISCUSSION

Resolution of the Rate Data

The formation of $CuBPEDA^{+2}$ from $NiBPEDA^{+2}$ and Cu^{+2} may proceed through either or both of two pathways as shown in equation 17.

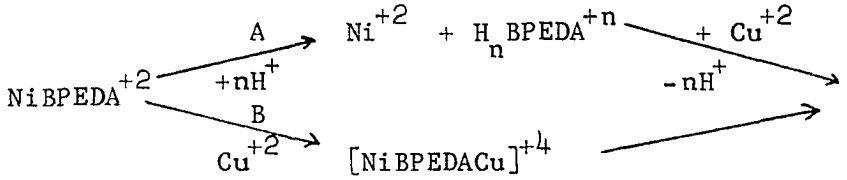

(17)

Pathway A represents a complete dissociation of $NiBPEDA^{+2}$ prior to copper attack. Protons will be involved in the dissociation due to the basicity of BPEDA. The rate determining step cannot be the copper attack on BPEDA due to the sluggish nature of Ni-ligand dissociation and the very rapid rate of formation of copper complexes. Pathway B involved a direct attack of copper on $NiBPEDA^{+2}$ and results in the formation of some type of dinuclear intermediate prior to complete dissociation of BPEDA from $NiBPEDA^{+2}$. Intermediates of this type are quite common in metal exchange studies involving aminocarboxylate ligands (1-6) although there have been only two studies showing similar intermediates involving polyamine ligands (10,11).

The contribution of pathway A to the total exchange rate can be calculated since the kinetics of the formation of $NiBPEDA^{+2}$ from Ni^{+2} and BPEDA, $HBPEDA^{+}$ and H_2BPEDA^{+2} has been studied (18) and the stability constant associated with each reaction can be calculated. Since these species have been shown to be kinetically important in the formation of $NiBPEDA^{+2}$, the dissociation of $NiBPEDA^{+2}$ must follow the

same pathway and the rate of dissociation at constant pH can be written as shown in equations 18 and 19.

$$d[NiL] = k_d[NiL] = k^{NiL}[NiL] + k_H^{NiL}[NiL][H^+] + k_{2H}^{NiL}[NiL][H]^2 \quad (18)$$

$$k_d = k^{NiL} + k_{2H^+}^{NiL}[H] + k_{2H^+}^{NiL}[H]^2 \quad (19)$$

Since

$$K_{NiL}^{Ni,L} = \frac{k_{Ni}^{L}}{k^{NiL}} \quad (20)$$

$$K_{NiL}^{Ni,HL} = \frac{K_{NiL}}{K_{HL}} = \frac{k_{Ni}^{HL}}{k_H^{NiL}} \quad (21)$$

$$K_{NiL}^{Ni,H_2L} = \frac{K_{NiL}}{K_{HL} \times K_{H_2L}} = \frac{k_{Ni}^{H_2L}}{k_{2H}^{NiL}} \quad (22)$$

values of k^{NiL}, k_H^{NiL} and k_{2H}^{NiL} can be calculated using the known values of formation rate constants and equilibrium constants listed in Table 9 and defined in the appendix. Thus,

$$k_d = 7.32 \times 10^{-12} sec^{-1} + 1.98 \times 10^{-4}[H^+] sec^{-1} + 25.8[H^+]^2 sec^{-1} \quad (23)$$

and equation 23 allows calculation of the contribution of pathway A to the overall exchange rate at each pH studied. The dissociation term, k_d, becomes negligible above pH 4.5. Below pH 4.5 the observed rate

TABLE 9

STABILITY CONSTANTS AND FORMATION RATE CONSTANTS FOR INDIVIDUAL SPECIES OF THE NiBPEDA^{+2} SYSTEM.

All values at 25° C and μ = 0.1 M

Reaction	K_{NiL}^{Ni,H_nL}	$k_{Ni}^{H_nL}$, $M^{-1}sec^{-1}$ [a]	K_{H_nL} [b]
$Ni^{+2} + L$	2.52×10^{14}	1.82×10^{3}	---
$Ni^{+2} + HL^{+}$	1.91×10^{8}	2.62×10^{2}	---
$Ni^{+2} + H_2L^{+2}$	2.96×10^{5}	1.15×10^{2}	---
$HL^{+} \longrightarrow H^{+} + L$	----	----	5.25×10^{-9}
$H_2L^{+2} \longrightarrow H^{+} + HL^{+}$	----	----	3.39×10^{-6}

a = reference 18

b = reference 14

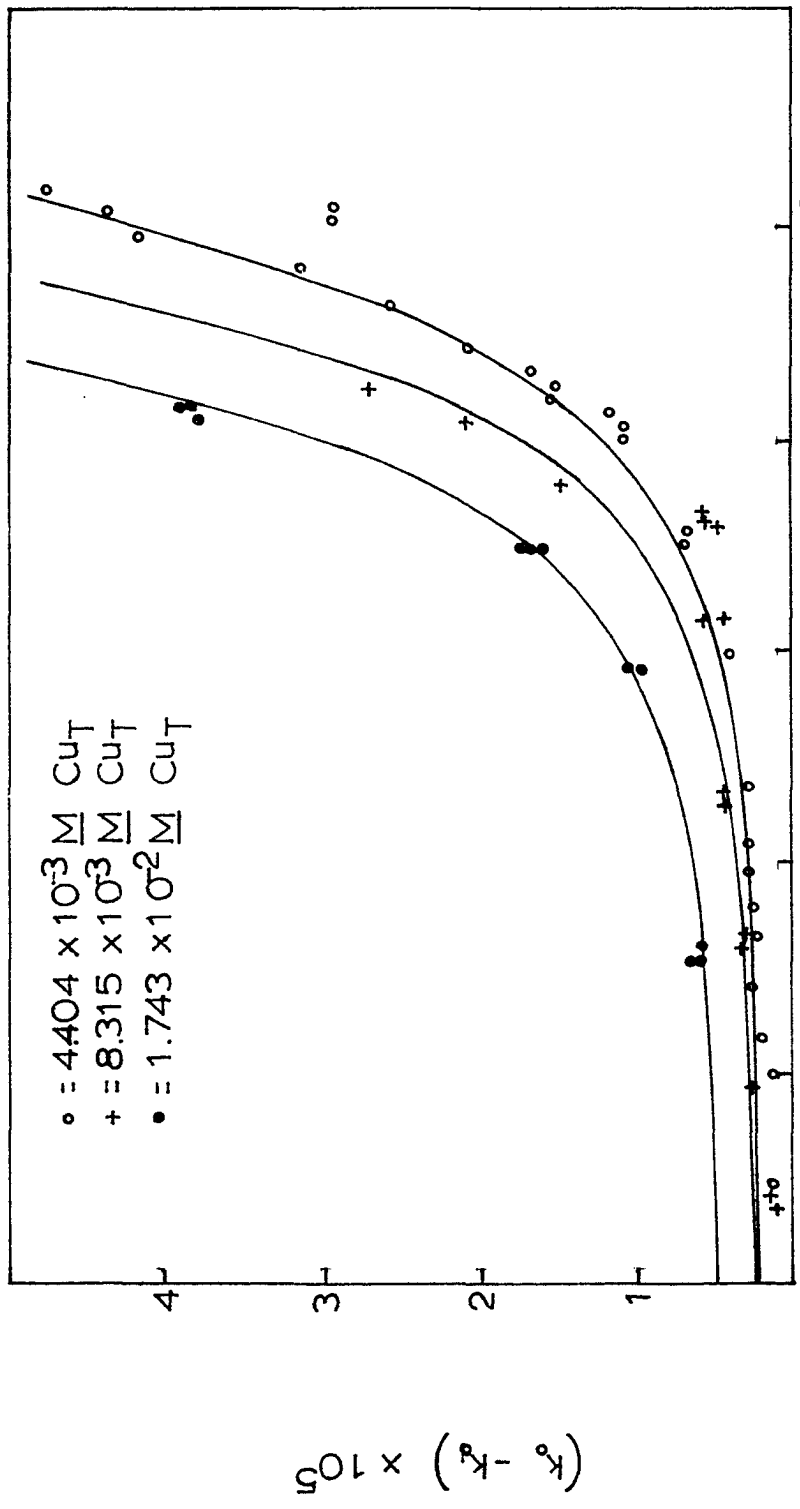

Figure 1. pH dependence of the rate of the exchange reaction.

constant, k_o, is corrected for the term by subtraction.

Pathway B involves a direct copper attack on partially dissociated $NiBPEDA^{+2}$. Further, plots of k_o-k_d against pH at constant total copper concentration, shown in Figure 1, indicate that the exchange reaction is pH sensitive since the rate increases greatly with increasing pH. The rate, however, varies inversely with $[H^+]$, not directly as would be expected if $[H^+]$ were attacking the partially dissociated BPEDA. Thus, the pH behavior rules out proton assisted dissociation. Actually, this is to be expected since the terminal dentate sites which are first to unwrap from $NiBPEDA^{+2}$ are pyridyl groups with pK_a values < 2. Further, no stable protonated complexes such as $NiBPEDAH^{+3}$, analogous to the known $Ni(trien)H^{+3}$, have been found.

One possible explanation for the inverse $[H^+]$ behavior would be the existence of hydroxy complexes of $NiBPEDA^{+2}$. Such species do exist in the case of $Ni(trien)^{+2}$ but only above pH 9 (19). It is most unlikely that replacement of two terminal aliphatic nitrogens by pyridyl groups could cause a shift in hydrolysis of 6 pK units. The other explanation for the inverse hydrogen ion effect involves the attack of hydrolyzed copper species on $NiBPEDA^{+2}$. There is both thermodynamic and kinetic evidence for their existence. Many hydrolyzed species have been proposed, for example $CuOH^+$, $Cu_2(OH)_2^{+2}$, $Cu_3(OH)_2^{+4}$, Cu_2OH^{+3} and $Cu_n(OH)_{2n-2}^{+2}$ (20-22). Only the existence and formation constant of $Cu_2(OH)_2^{+2}$ is well documented and agreed upon, although the existence of $CuOH^+$ is accepted by all workers except Perrin (21). Assuming the

existence and kinetic activity of $CuOH^+$ and $Cu_2(OH)_2^{+2}$ to be the explanation for the pH behavior seen, equation 24 can be written.

$$(k_o - k_d)[NiBPEDA^{+2}] = k_{Cu^{+2}}^{NiL}[Cu^{+2}][NiBPEDA^{+2}]$$

$$+ (k_{CuOH^+}^{NiL})[CuOH^+][NiBPEDA^{+2}] + (k_{Cu_2(OH)_2^{+2}}^{NiL})[Cu_2(OH)_2][NiBPEDA^{+2}] \quad (24)$$

By use of the relations

$$\beta_{11} = \frac{[CuOH^+][H^+]}{[Cu^{+2}]} \quad (25)$$

and

$$\beta_{22} = \frac{[Cu_2(OH)_2^{+2}][H^+]^2}{[Cu^{+2}]^2} \quad (26)$$

equation 24 may be rewritten as

$$k_o - k_d = (k_{Cu^{+2}}^{NiL} + k_{CuOH^+}^{NiL} \frac{\beta_{11}}{[H^+]}$$

$$+ k_{Cu_2(OH)_2^{+2}}^{NiL} \beta_{22} \frac{[Cu^{+2}]}{[H^+]^2}) \quad [Cu^{+2}] \quad (27)$$

The free copper concentration at any pH and total copper concentration can be calculated from equation 28 using known values of the formation constants for each species corrected to 0.1 M ionic strength. The corrected values are $\beta_{11} = 5.0 \times 10^{-8}$, $\beta_{21} = 1.4 \times 10^{-6}$, and $\beta_{22} = 2.5 \times 10^{-11}$ which are derived from the values determined by Ohtaki and

Kawai (20).

$$[Cu]_{total} = [Cu^{+2}] + [CuOH^{+}] + 2[Cu_2OH^{+3}] + 2[Cu_2(OH)_2^{+2}] \quad (28)$$

The term $Cu_3(OH)_2^{+4}$ was included originally but represents only a small fraction of $[Cu]_{total}$ particularly at low total copper concentrations and so was dropped from subsequent calculations. Figure 2 shows the distribution of copper species as a function of pH at two total copper concentrations.

At low pH and low total copper concentrations dimerization is slight and the last term on the right hand side of equation 27 can be neglected for a first approximation of $k_{Cu^{+2}}^{NiL}$. Equation 27 then rearranges to

$$\frac{k_o - k_d}{[Cu^{+2}]} = k_{Cu^{+2}}^{NiL} + k_2\beta_{11}\frac{1}{[H^{+}]} \quad (29)$$

Figure 3 shows a least squares plot of equation 29 for the pH range 3.7 to 4.5 using the calculated values of $[Cu^{+2}]$ at a constant total copper concentration of 4.404×10^{-3} M. The intercept yields a first estimate value of $k_{Cu^{+2}}^{NiL} = 4.92 \times 10^{-4}\ M^{-1}sec^{-1}$. This value can be inserted in equation 27 and the equation rearranged as in equation 30 and plotted as shown in Figure 4 for the pH range 4.9 to 6.1 again at total copper concentration of 4.404×10^{-3} M.

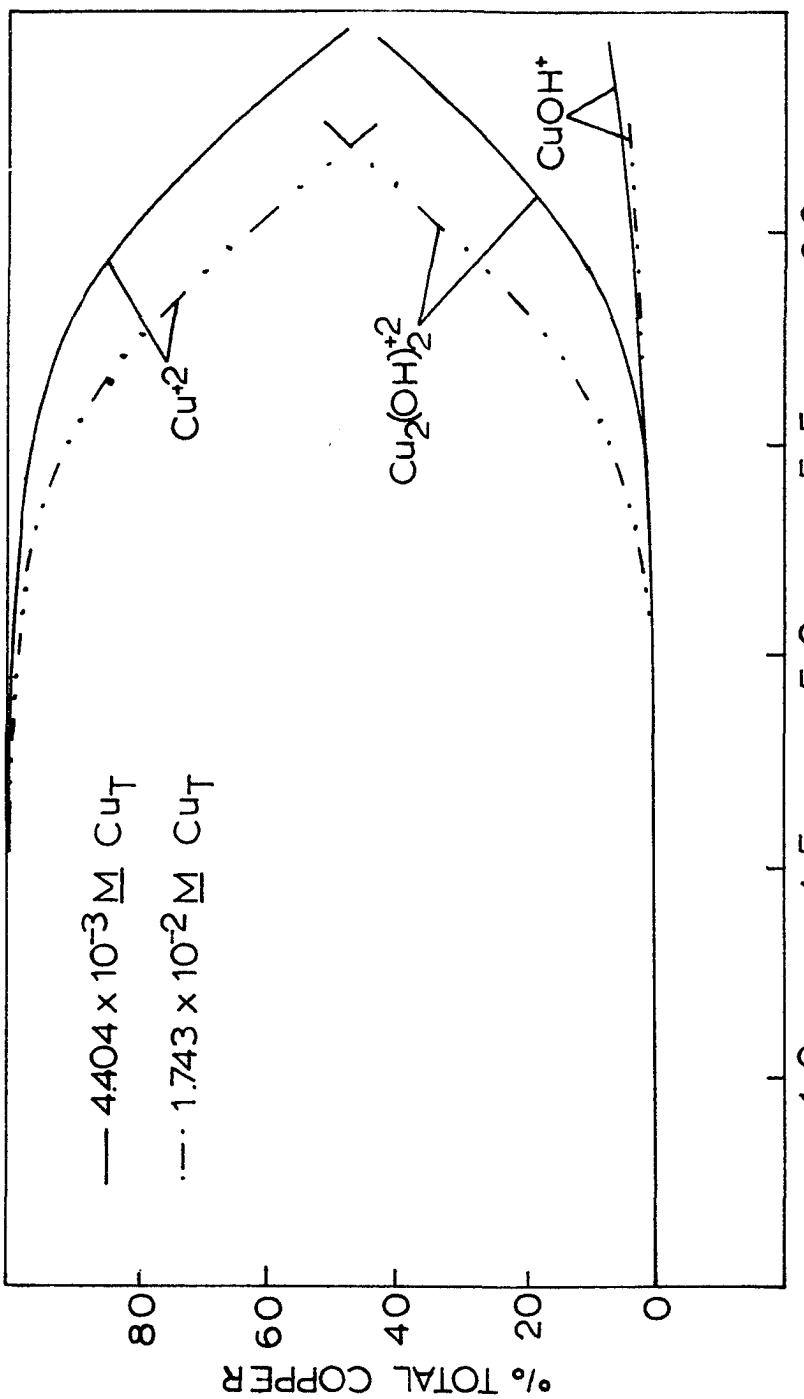

Figure 2. Distribution of copper species as a function of pH.

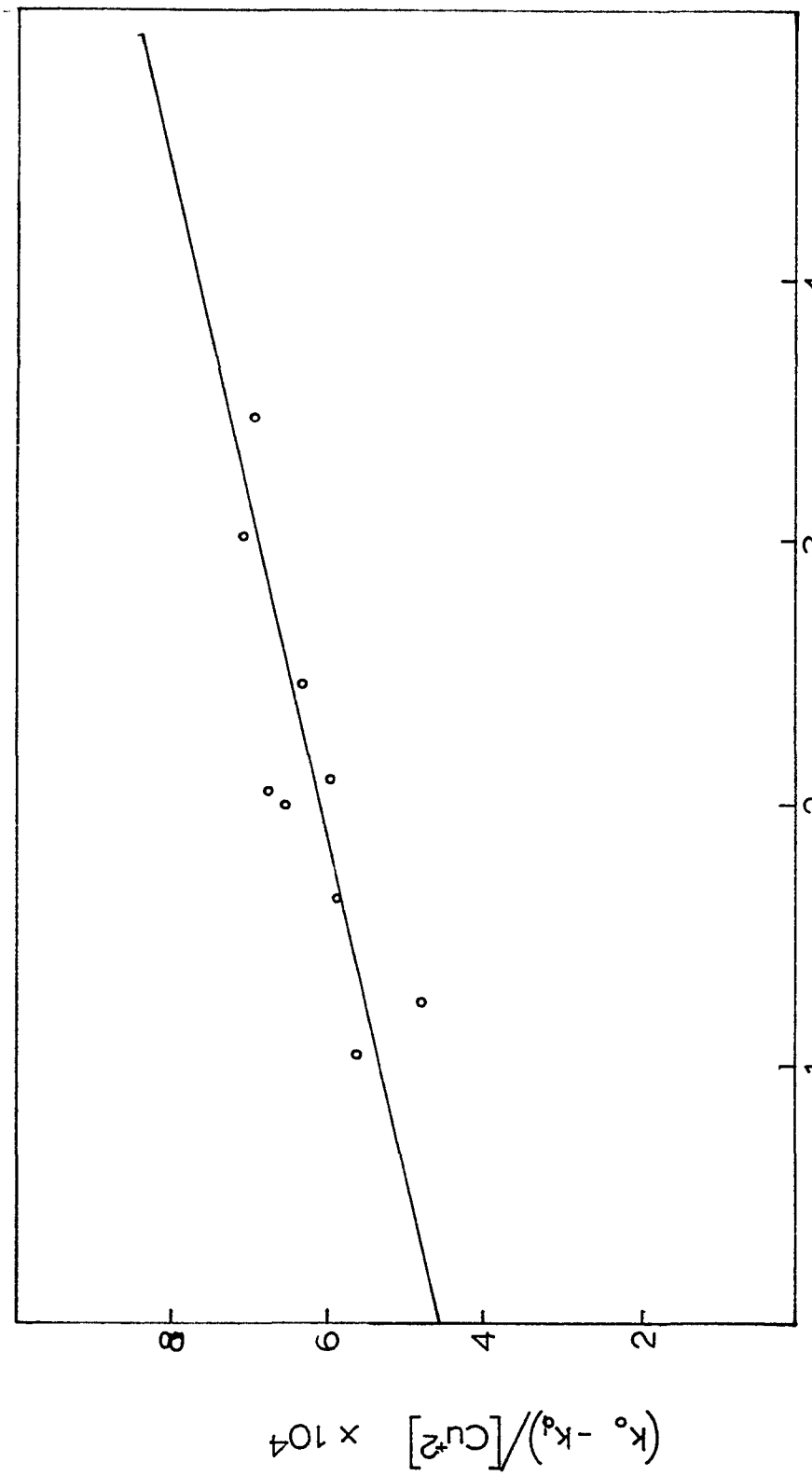

Figure 3. Initial resolution of rate constant $k^{NiL}_{Cu^{+2}}$. Data from exchange at total copper concentration of 4.404×10^{-3} M.

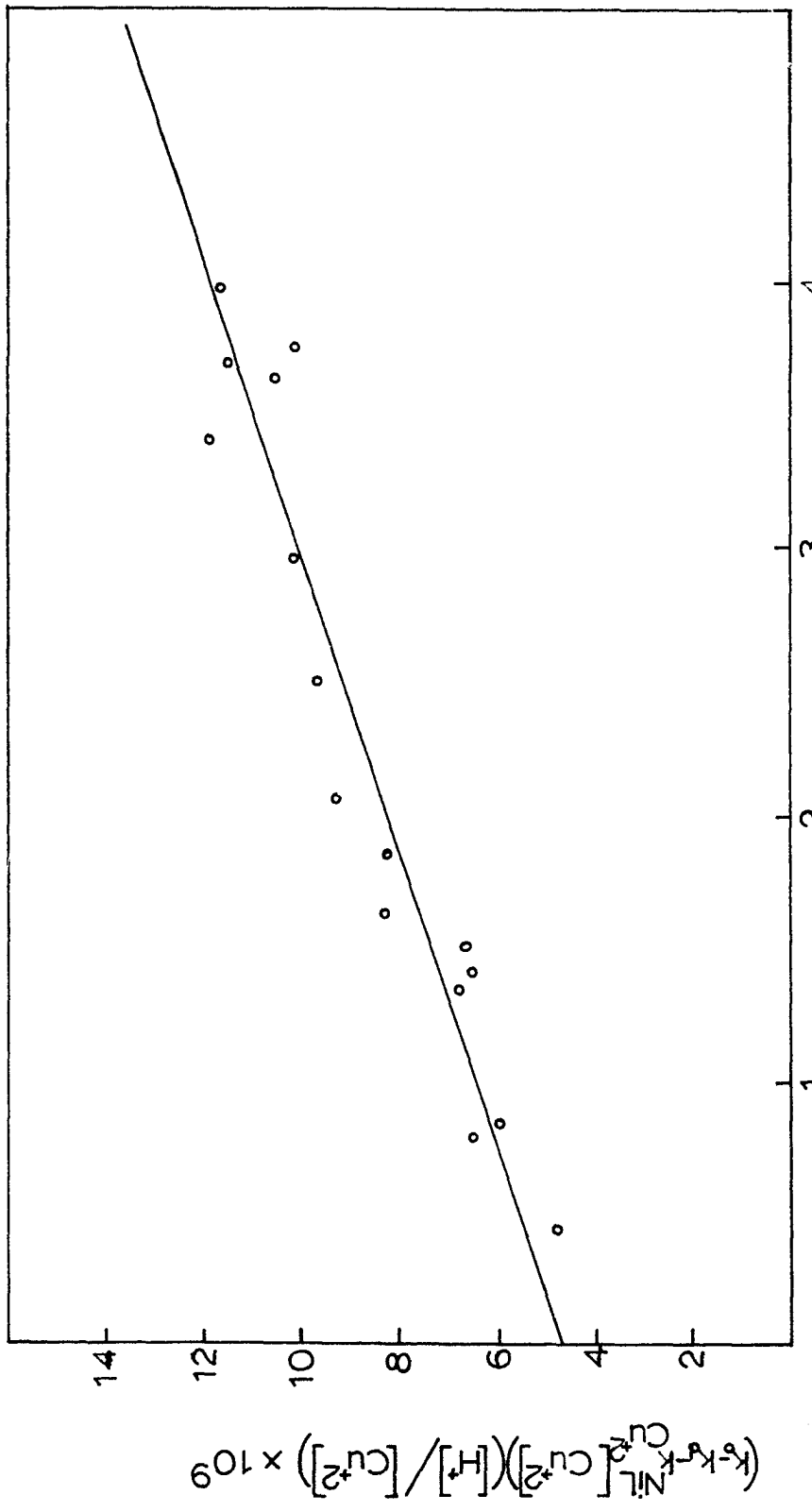

Figure 4. Resolution of rate constant $k_{Cu_2(OH)_2^{+2}}^{NiL}$. Data from exchange at total copper concentration of 4.404×10^{-3} M.

$$(k_o - k_d - k^{NiL}_{Cu^{+2}}[Cu^{+2}])\ \frac{[H^+]}{[Cu^{+2}]} = (k^{NiL}_{CuOH^+})\beta_{11} + (k^{NiL}_{Cu_2(OH)_2^{+2}})\ \frac{[Cu^{+2}]}{[H^+]}\ \beta_{22} \quad (30)$$

The slope and β_{22} yielded a value of $7.237 \times 10^{-2}\underline{M}^{-1}sec^{-1}$ for $k^{NiL}_{Cu_2(OH)_2^{+2}}$. Substitution of this value into equation 27, rearranging as in equation 31 and plotting

$$\left\{ k_o - k_d - k^{NiL}_{Cu_2(OH)_2^{+2}}[Cu_2(OH)_2^{+2}] \right\} / [Cu^{+2}] = k^{NiL}_{Cu^{+2}} + (k^{NiL}_{CuOH^+})\beta_{11}\ \frac{1}{[H^+]} \quad (31)$$

over the same pH range as Figure 3 yielded values of $4.975 \times 10^{-4}\underline{M}^{-1}sec^{-1}$ and $0.1080\ \underline{M}^{-1}sec^{-1}$ for $k^{NiL}_{Cu^{+2}}$ and $k^{NiL}_{CuOH^+}$, respectively.

Since $Cu_2(OH)_2^{+2}$ is a dimer of $CuOH^+$ equation 32 could explain the pH behavior with only Cu^{+2} and $CuOH^+$ as reactive species.

$$k_o - k_d = k^{NiL}_{Cu^{+2}}[Cu^{+2}] + k^{NiL}_{CuOH^+}\ ([CuOH^+] + 2[Cu_2(OH)_2^{+2}]) \quad (32)$$

$$= k^{NiL}_{Cu^{+2}}[Cu^{+2}] + k^{NiL}_{CuOH^+}\ ([CuOH^+]\ \left\{ 1 + 2[CuOH^+]\ \frac{\beta_{22}}{\beta_{11}^2} \right\}\ ). \quad (33)$$

A plot of $(k_o - k_d)/[Cu^{+2}]$ against $([CuOH^+]\ \left\{ 1 + 2[CuOH^+]\ \frac{\beta_{22}}{\beta_{11}^2} \right\})/[Cu^{+2}]$, shown in Figure 5, covering the pH range 3.7 to 6.1 with the total copper concentration at $4.404 \times 10^{-3}\underline{M}$

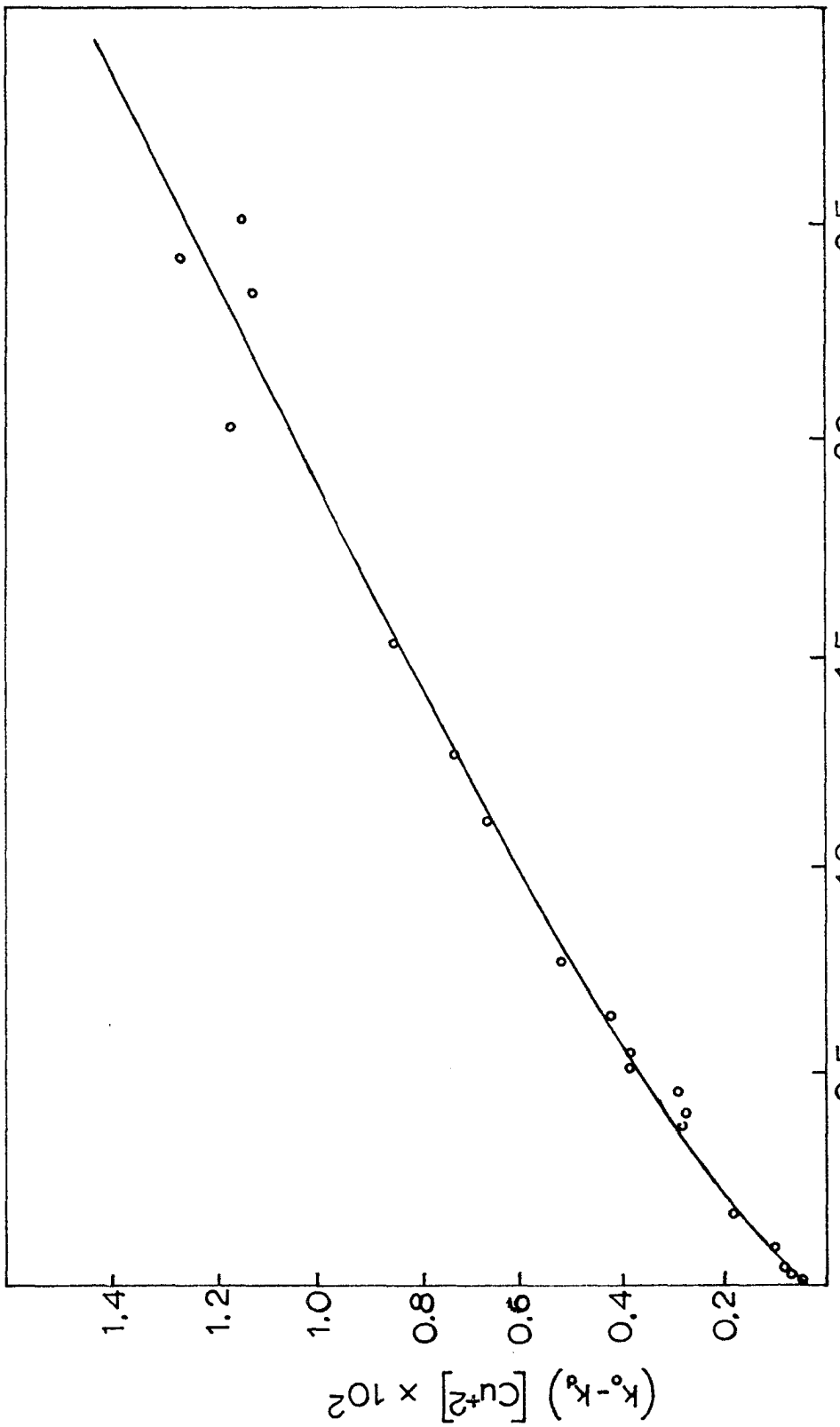

Figure 5. Non-linear plot demonstrating that $CuOH^+$ and $Cu_2(OH)_2^{+2}$ are individual species.

is not linear. Thus, $Cu_2(OH)_2^{+2}$ is a reactive species.

The resolved values of $k^{NiL}_{Cu^{+2}}$, $k^{NiL}_{CuOH^+}$ and $k^{NiL}_{Cu_2(OH)_2^{+2}}$ along with k_d can be used to construct a theoretical curve of k_o against pH from equation 24 at a total copper concentration of 4.404×10^{-3} M. A computer generated curve is compared to the experimentally determined values in Figure 6. Excellent agreement is seen over the entire pH range. However, calculated values of k_o from equation 24 at higher copper concentrations show marked deviation from the experimental values. Comparisons of the experimentally determined points to the theoretical curves generated by a computer at total copper concentrations of 8.315×10^{-3} M and 1.743×10^{-2} M are shown in Figures 7 and 8 respectively. In all cases, the predicted k_o values are higher than the experimental ones. The most likely explanation for this behavior is the existence of higher order polynuclear hydrolyzed copper species such as those proposed by Perrin, $Cu_n(OH)^{+2}_{2n-2}$. These species have not been characterized but would become important at both higher total copper and higher pH and thus lower the concentrations of Cu^{+2}, $CuOH^+$ and $Cu_2(OH)_2^{+2}$ which would cause lower experimental values of k_o. The actual free copper present at higher total copper concentrations can be calculated using equation 27 and the resolved values of $k^{NiL}_{Cu^{+2}}$, $k^{NiL}_{CuOH^+}$, $k^{NiL}_{Cu_2(OH)_2^{+2}}$ and k_o and k_d. Attempts at relating these values to higher order polynuclear hydrolyzed copper species using equations resembling equations 25, 26 and 28 failed.

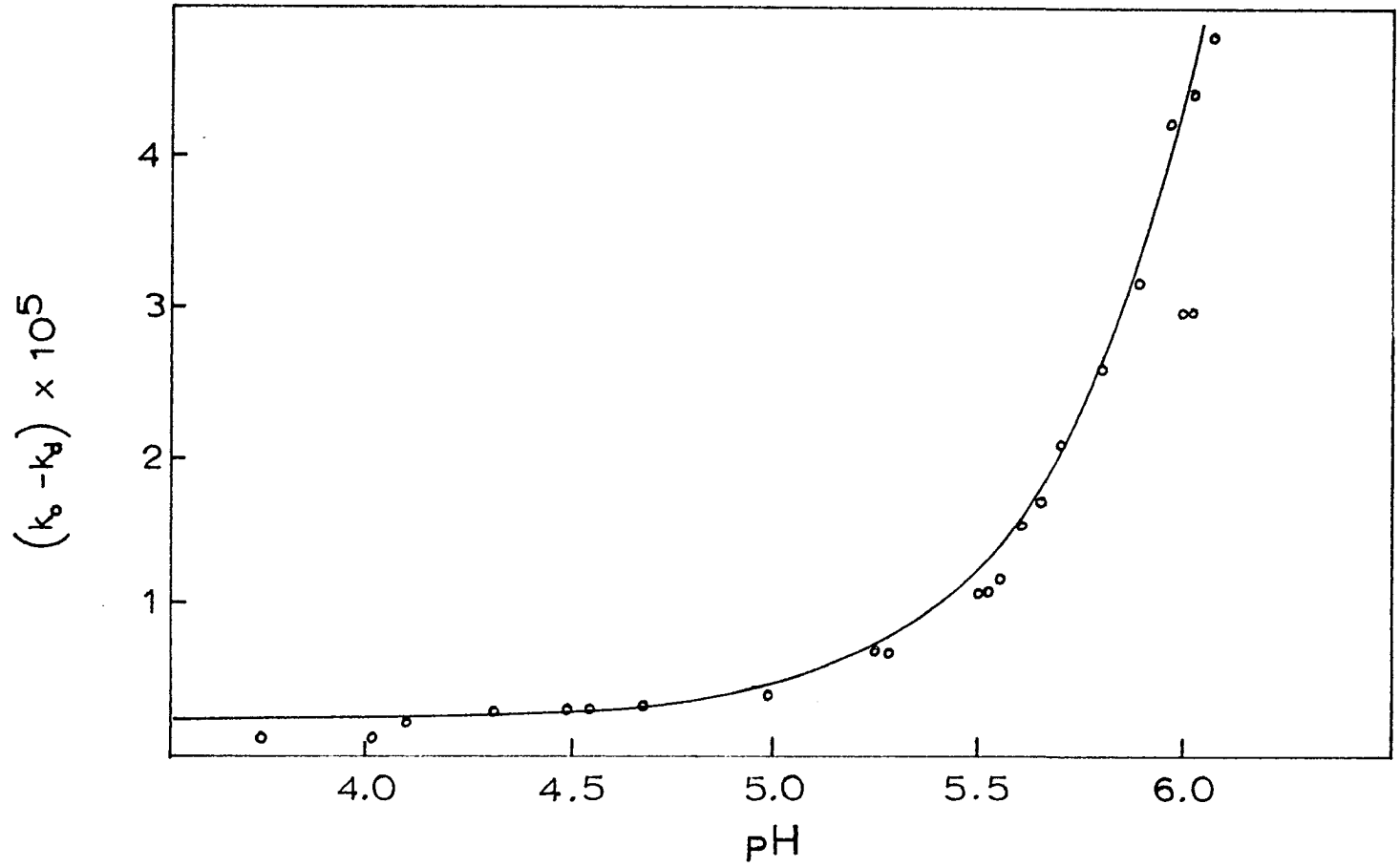

Figure 6. Comparison of theoretical curve to experimentally determined values of $k_o - k_d$ at total copper concentration = 4.404×10^{-3} M.

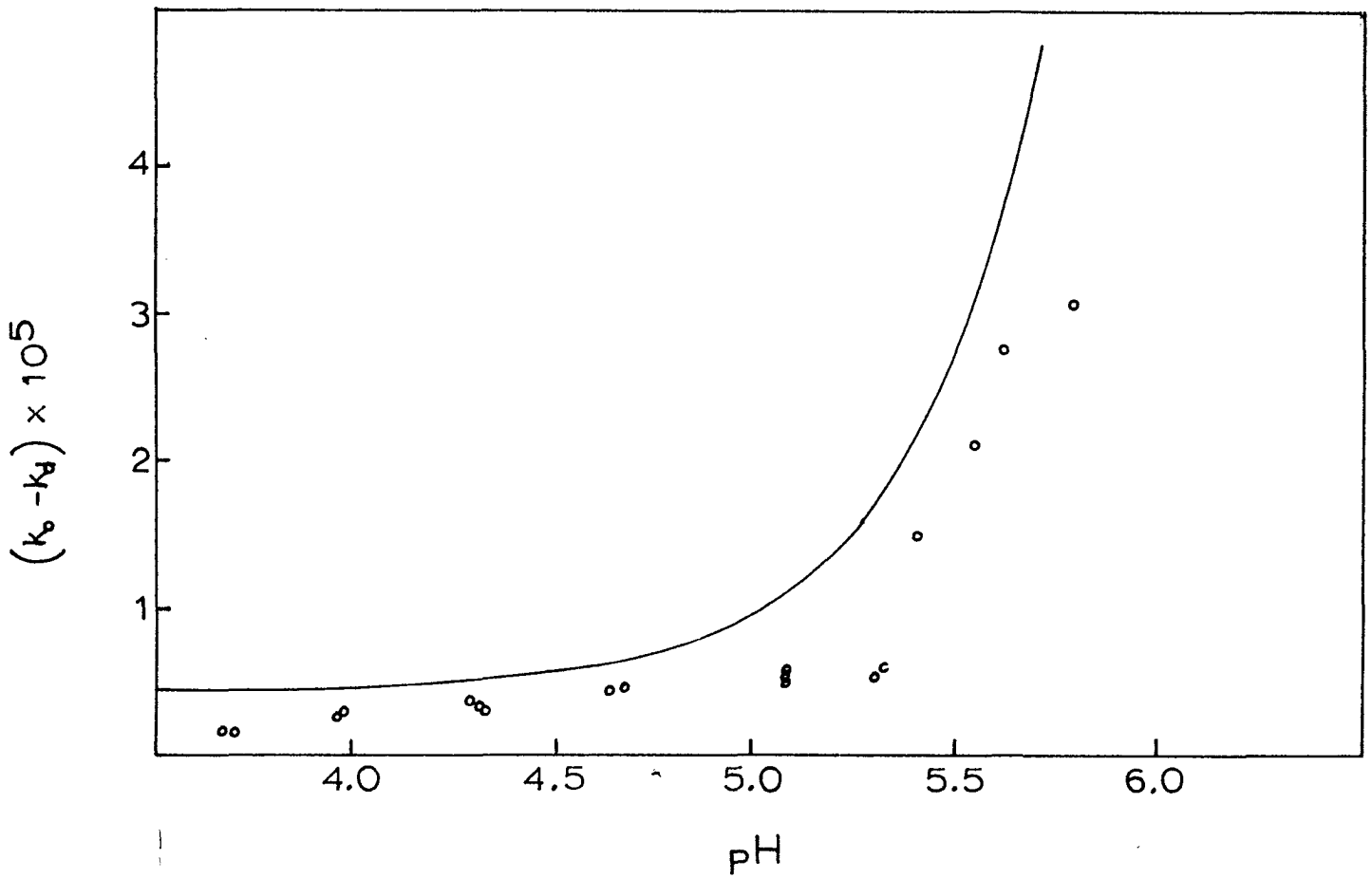

Figure 7. Comparison of theoretical curve to experimentally determined values of $k_o - k_d$ at total copper concentration = 8.315×10^{-3} M.

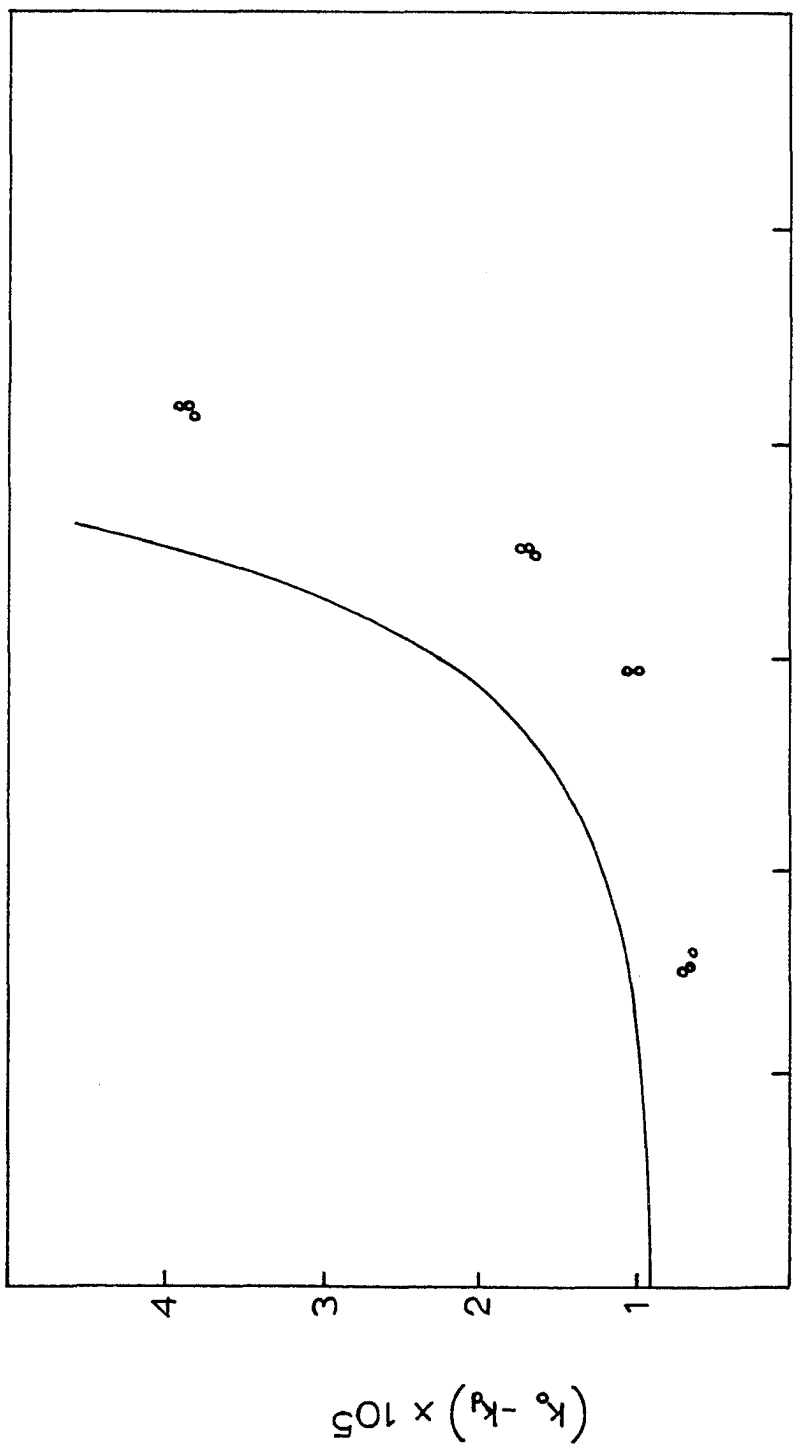

Figure 8. Comparison of theoretical curve to experimentally determined values of $k_o - k_d$ at total copper concentration = 1.743×10^{-2} M.

Mechanism of the Exchange Reaction

The resolved rate constants show the exchange reaction, corrected for dissociation, to be first order in a copper species in each case. Thus, copper must be involved either during or before the rate determining step and clearly prior to complete dissociation of $NiBPEDA^{+2}$. The transfer of BPEDA from Ni^{+2} to Cu^{+2}, analogous to all other dissociation and exchange reactions, most likely proceeds in a stepwise sequence of bond rupture with the departing metal and bond formation, limited by water loss, to the attacking metal. Due to the extreme lability of the copper formation reaction, $k^{-H_2O} = 3 \times 10^8\ sec^{-1}$ (23), and the pronounced sluggish rate of exchange seen in this study, pure bond formation to copper cannot be rate limiting.

The proposed mechanism involves stepwise dissociation of BPEDA from Ni^{+2}, followed by coordination of free dentate sites to copper where sterically possible. This gives rise to a series of dinuclear intermediates having one of the dissociation steps along the series as rate determining.

An analysis of the reaction mechanism involves a knowledge of the stability constants of the nucleophile with various ligands. Since these values are known for nickel and copper, but not for hydrolyzed copper species, only the term and pathway involving free copper will be analyzed in detail.

Previous metal exchange studies have shown that the nature of the dinuclear intermediate immediately prior to the rate determining step may be characterized by comparison to other similar systems. The ratio

of experimental rate constants for metal attack is directly proportional to the ratio of the dinuclear intermediate stability constants provided the same rate determining step holds for both systems (3,4,6). Thus, if a series of dinuclear intermediates are possible, each with a different stability constant, the one whose constant gives the closest agreement in comparison to a known system to the ratio of experimental rate constants is the intermediate immediately prior to the rate determining step.

The systems chosen for comparison are the copper exchange with NiEDDA (8), with $Ni(trien)^{+2}$ (11) and with $NiEDTA^{-2}$ (7). In all of these systems, the rate determining step has been shown to be the breakage of a nickel-aliphatic nitrogen bond. In the present study both aromatic and aliphatic nitrogens are involved, and some possible intermediates involve nickel-aromatic bond rupture. Since intermediates are compared to systems having nickel-aliphatic nitrogen bond rupture, a correction for the increased lability of nickel aromatic bond is needed. The ratio of the rate of dissociation of Ni-pyridine to Ni-ammonia represents this difference and amounts to a factor of 5.

Equation 34 shows the comparison with L representing any ligand, and K_R the relative stability constant of the intermediate immediately prior to the rate determining step.

$$\frac{k_{Cu}^{NiBPEDA}}{k_{Cu}^{NiL}} = \frac{K_R^{NiBPEDA-Cu}}{K_R^{NiL-Cu}} \qquad (34)$$

The relative stability constant, K_R, of each intermediate structure for each system can be defined in terms of the stability of the

Ni-ligand and Cu-ligand segments involved as compared to the stability of the initial complex.

$$K_R = \frac{(K_{Ni\text{-}segment})(K_{Cu\text{-}segment})}{K_{Ni\text{-}complex}} \qquad (35)$$

In some comparisons an electrostatic attraction helps stabilize one intermediate relative to the other. The added stability of this contribution, K_{el}, can be estimated using equation 36

$$\Delta E_{electrostatic} = \frac{Z_A Z_B e^2}{Dr_{AB}} = 2.303\ RT \log K_{el} \qquad (36)$$

where Z_A and Z_B are the charges involved, D is the dielectric constant of water, r_{AB} is the distance of separation between A and B, T is the temperature in ^oK and R is the gas constant.

There may also be a statistical factor which favors the formation of one intermediate relative to another and this term must be included in making comparisons.

A comparison of possible likely dinuclear intermediates for the exchange of $NiBPEDA^{+2}$ with Cu^{+2} to the known systems previously mentioned is made in Table 10. Values of K_R, K_{el} and statistical factors are included. The last row in Table 10 shows the ratio of experimental rate constants. The values of K_R were calculated from known stability constants chosen to be as internally consistent as possible with respect to temperature and ionic strength and are listed in Table 11 along with experimental values of the rate constants. A comparison of the ratio of experimental rate constants to the predicted ratios of intermediate

TABLE 10

COMPARISON OF POSSIBLE DINUCLEAR INTERMEDIATES FOR THE EXCHANGE OF $NiBPEDA^{+2}$ WITH Cu^{+2} TO KNOWN SYSTEMS.

Nitrien-Cu	NiEDDA-Cu	NiEDTA-Cu
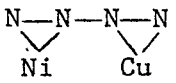	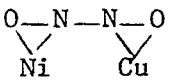	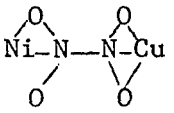
$K_R = 8$	$K_R = 4 \times 10^{-1}$	$K_R = 6 \times 10^{-3}$ Statistical factor = 2 $K_{el} = 3.16$

NiBPEDA-Cu Structure	K_R	$\frac{K_R^{NiBPEDA-Cu}}{K_R^{Nitrien-Cu}}$	$\frac{K_R^{NiBPEDA-Cu}}{K_R^{NiEDDA-Cu}}$	$\frac{K_R^{NiBPEDA-Cu}}{K_R^{NiEDTA-Cu}}$ [a]
I 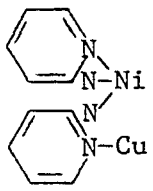	8×10^{-1}	1×10^{-1}	2	2×10^{1}
II 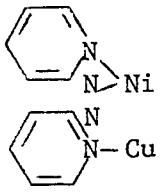	2×10^{-5}	2×10^{-6}	4×10^{-5}	4×10^{-4}
III 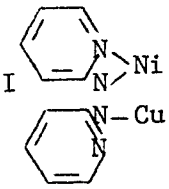	1×10^{-3}	1.5×10^{-4}	3×10^{-3}	3×10^{-2}

TABLE 10 (cont.)

IV 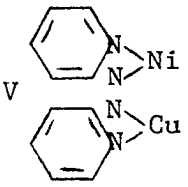	3×10^{2}	3×10^{1}	8×10^{2}	8×10^{3}
V 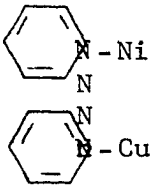	6×10^{-13}	4×10^{-13}[b]	1×10^{-11}[b]	1×10^{-10}[b]
VI 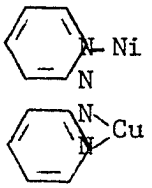	5×10^{-3}	3×10^{-3}[b]	5×10^{-2}[b]	5×10^{-1}[b]
VII 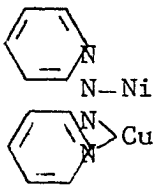	8×10^{-3}	1×10^{-3}	2×10^{-2}	2×10^{-1}
VIII 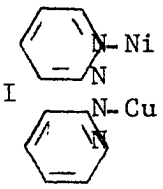	1×10^{2}	5×10^{1}[b]	2×10^{3}[b]	2×10^{5}[b]
$\frac{k_{Cu}^{NiBPEDA}}{k_{Cu}^{NiL}}$		2×10^{-4}	7×10^{-3}[c]	6×10^{-3}

[a] The statistical factor of 2 and the $K_{el} = 3.16$ are figured into this value of $K_{R}^{NiEDTA-Cu}$.

[b] Values include a factor of 5 for the ratio of Ni-NH_3 to Ni-py bond breakage.

[c] This ratio is somewhat high due to k_{Cu}^{NiEDDA} being measured at μ=1.25 M.

TABLE 10 (cont.)

The value of k_{Cu}^{NiEDTA} increases by 5 in going from μ = 1.25 to 0.1 M. Thus k_{Cu}^{NiEDDA} would also increase making the ratio smaller.

TABLE 11

STABILITY CONSTANTS AND RATE CONSTANTS USED IN MAKING COMPARISONS SHOWN IN TABLE 10.

All values are either at 25° C and μ = 0.1 M or chosen to be as close to these conditions as possible.[a]

Ligand	Log $K_{NiL}^{Ni,L}$	Log $K_{CuL}^{Cu,L}$	k_{Ni}^{CuL}, $M^{-1}sec^{-1}$
BPEDA	14.4[b]	---	4.9×10^{-4}[c,d]
EDDA	13.5	---	$7. \times 10^{-2}$[e]
EDTA	18.6	---	7.5×10^{-2}
trien	14.1	---	2.7[f]
AMP	7.2	9.6	
AEAMP	11.9[c]	14.6[g]	
en	7.5	10.6	
dien	10.7	16.0	
glycine	5.3	7.6	
IDA	---	11.1	
NH_3	2.7	4.3	
pyridine	1.8	2.4	

[a] Except as noted all values taken from reference 24.

[b] Reference 14.

[c] This work.

[d] Reference 8.

[e] Reference 1.

[f] Reference 11.

[g] Reference 15.

stability constants, shows that structures III and VII give predicted values which agree closely to the experimental rate constant ratios in all cases. Other structures listed in the Table as well as some not listed were tested and gave values which are off by orders of magnitude.

Of the two possible intermediate structures, VII involves dissociation of BPEDA at both ends with an AMP segment chelated to copper and at the opposite end of the complex a free pyridyl group. This is highly unlikely since stability constants of nickel with aromatic-aliphatic mixed ligands show little loss and in some cases a gain by replacing an aliphatic nitrogen by an aromatic one. The values are listed in Table 12. Thus, there appears to be no strain in the bonding of an AMP segment to nickel and therefore, no reason for it to dissociate in a manner such as structure VII. Structure III, however, is not without its peculiarities in that here copper is bonded to an internal aliphatic nitrogen and not chelated to the pyridyl group. Unlike nickel, the replacement of an aliphatic nitrogen with an aromatic one does markedly decrease the stability of copper complexes. In fact, Cudien, $K = 10^{16}$, is practically as stable as CuBPEDA, $K = 10^{16.3}$. Table 12 shows the comparisons. Thus, it is not unreasonable to suggest some type of strain or hindrance which prevents copper from chelating to the free AMP segment of BPEDA. Finally, structure III does give the best agreement to the ratio of experimental rate constants.

On this basis a mechanism for the metal exchange of $NiBPEDA^{+2}$ and copper can be proposed. This is shown in Figure 9. As previously discussed, nickel-nitrogen bond breakage is the rate determining step,

TABLE 12

COMPARISON OF STABILITY CONSTANTS BETWEEN ALIPHATIC AND AROMATIC NITROGEN COMPLEXES WITH NICKEL (II) AND COPPER (II).

All values at 25° C and μ = 0.1 M

Copper

Ligand	Log $K^{Cu,L}_{CuL}$	(Log $K_{aliphatic}$ - Log $K_{aromatic}$)	Ref.
NH_3	4.3		24
pyridine	2.4	+1.9	24
en	10.6		24
AMP	9.6	+1.0	24
dien	16.0		24
AEAMP	14.6	+1.4	15
trien	20.5		24
BPEDA	16.3	+4.2	14
	Nickel		
NH_3	2.7		24
pyridine	1.8	+0.9	24
en	7.5		24
AMP	7.2	+0.3	24
dien	10.7		24
AEAMP	11.9	-1.2	This work
trien	14.1		24
BPEDA	14.4	-0.3	14

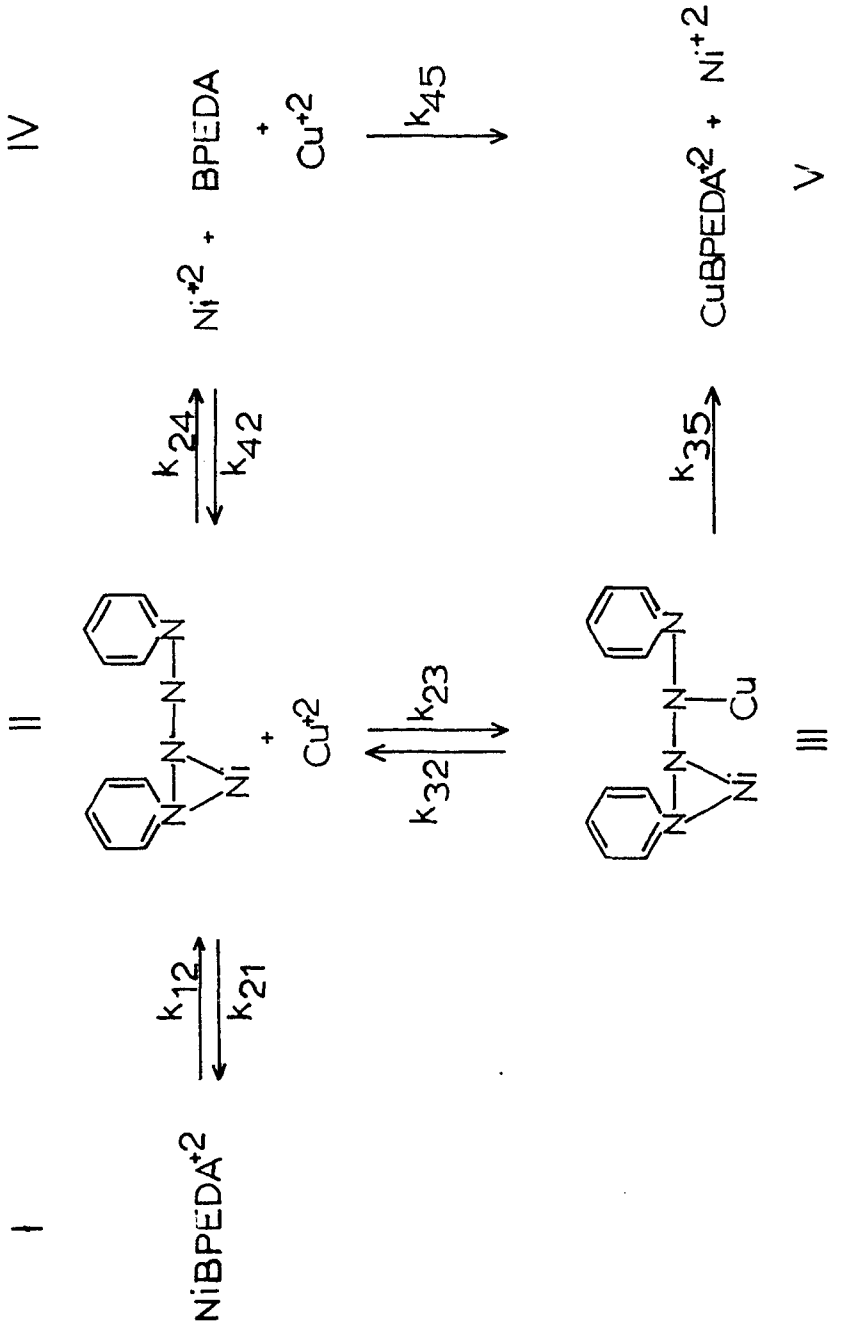

Figure 9. Mechanism for the reaction of Cu^{+2} with $NiBPEDA^{+2}$.

immediately following intermediate III. Further, the sequence I→ II→IV→V is nearly negligible and can be corrected for from prior knowledge of the dissociation of $NiBPEDA^{+2}$.

The copper dependent exchange pathway in Figure 9 must be I→ II→ III→ V. A general kinetic expression for the pathway can be written by assuming the steady-state approximation for species II and III.

$$[II] = \frac{k_{12}[I] + k_{32}[III]}{k_{21} + k_{23}[Cu^{+2}]} \tag{37}$$

$$[III] = \frac{k_{23}[Cu^{+2}][II]}{k_{32} + k_{35}} \tag{38}$$

$$k_o = \frac{k_{12}k_{23}k_{35}[Cu^{+2}]}{k_{21}k_{32} + k_{21}k_{35} + k_{23}k_{35}[Cu^{+2}]} \tag{39}$$

Expression 39 reduces to 40 since $k_{21}k_{32} \gg k_{21}k_{35}$ and $> k_{23}k_{35}[Cu^{+2}]$ at $[Cu^{+2}] \leq 10^{-2}$ M.

$$k_o = k^{NiBPEDA}_{Cu^{+2}}[Cu^{+2}] = \frac{k_{12}k_{23}k_{35}[Cu^{+2}]}{k_{21}k_{32}} \tag{40}$$

Thus, the expression derived from the proposed mechanism fits the experimental behavior.

Confirmation of the structure of species III in Table 10 may now be obtained knowing the kinetic expression for the mechanism. It is

possible to predict the value of $k^{NiBPEDA}_{Cu^{+2}}$ from the relative stability constant of species III and an accurate value of k_{35}. This assumes, as seen in equation 40, that the steps prior to the rate determining step are essentially in equilibrium and equation 40 can be written as

$$k^{NiBPEDA}_{Cu^{+2}} = K_R k_{35} \qquad (41)$$

The value of K_R is 1.2×10^{-3} for species III. An accurate estimate of k_{35} can be obtained from the hydrogen assisted dissociation of Ni(N-pren), where N-pren is $NH_2CH_2CH_2NHCH_2CH_3CH_3$. Under strongly acidic conditions protonation of the secondary nitrogen occurs immediately upon bond rupture making the first bond rupture rate determining rather than the last (25). Thus, $k_{35} = 3 \times 10^{-1} sec^{-1}$ and $k^{NiBPEDA}_{Cu^{+2}} = 1.2 \times 10^{-3} \times 3 \times 10^{-1} = 4 \times 10^{-4}\ \underline{M}^{-1}sec^{-1}$. The agreement between this predicted value and the experimentally observed one, $4.9 \times 10^{-4}\underline{M}^{-1}sec^{-1}$ is excellent. It may be noted that this calculation ignores the obvious accelerating effect that copper would have on k_{35} due to electrostatic interaction with nickel. However, also ignored is the decrease in K_R due to the same electrostatic interaction. It has been estimated (11) that these terms offset each other in the analogous $Ni(trien)^{+2}$ copper exchange and there is no reason not to believe the same is true in the present study.

The pathways involving $CuOH^+$ and $Cu_2(OH)_2^{+2}$ represent a problem and can be explained several ways. The accelerating effect of hydroxide has been seen in other systems but never explained in a satis-

factory fashion (9,10,11). If the same mechanism proposed for free copper is assumed to hold, then the enhancement in rate must be due only to an increase in the relative stability of intermediate III. This is not uncommon as numerous examples can be found illustrating an increase in stability for reactions such as equation 43.

$$CuL + OH^- \rightleftharpoons CuLOH^- \qquad (43)$$

Those pertinent to the present system are listed in Table 13. In all cases however, the addition of a hydroxide to the complex increases the stability by between 10^4 and 10^5, but the use of $CuOH^+$ as a reactant decreases the stability by 10^8. Therefore overall there is not a net gain, but a loss in stability due to $CuOH^+$ of about 10^2. In order to explain the increase in rate the stability should increase.

A second possibility is to assume that intermediate III is a transition state rather than an intermediate. If this is true, then an increase in the rate of water loss from copper due to hydroxide could increase the reaction rate. An increased lability of coordination compounds due to hydroxide has been seen with Co(III), Cr(III) and Fe(III) compounds and on this basis might be expected for Cu(II). However, it is known that there are two values of the rate of water loss for copper due to the Jahn-Teller effect; axial, which is rapid, and equatorial, which is sluggish. Further, it is argued that loss of axial water followed by ligand insertion in the inner coordination sphere is then immediately followed by a rapid internal interconversion of axial and equatorial sites (30). Not until three coordination sites

TABLE 13

EFFECT OF HYDROXIDE ON STABILITY OF COPPER (II) COMPLEXES.

Reaction	Log K_{stab}	Reference
$Cu(en)_2^{+2} + OH^- \longrightarrow Cu(en)_2OH^+$	5.8	26
$CuDMEN^{+2} + OH^- \longrightarrow Cu(DMEN)OH^+$	5.9	27
$Cudien^{+2} + OH^- \longrightarrow Cu(dien)OH^+$	5.0	28
$CuHEEN^{+2} + OH^- \longrightarrow Cu(HEEN)OH^+$	6.7	28
$Cutrien^{+2} + OH^- \longrightarrow Cu(trien)OH^+$	3.8	29

en = ethylenediamine

DMEN = N,N'-dimethylethylenediamine

dien = diethylenetriamine

HEEN = N-(2-hydroxyethyl)ethylenediamine

trien = triethylenetetramine

are occupied by ligands does copper exhibit a sluggish formation rate. Thus, it is suggested that the presence of an equatorial hydroxide, $CuOH^{+}$, will not greatly affect the rate at which axial water is lost. As further evidence for this, a study of the formation of mixed ligand species from Ni(5-x,phen) and dien or NTA showed the effect of the substituents to be transmitted to equatorial sites three times greater than to axial sites (31). Unlike copper, all six sites in nickel are initially approximately equal.

The third possibility is the formation of some type of hydrogen bonded intermediate or hydroxide bridge intermediate. The hydroxide oxygen could hydrogen bond to a proton of one of the waters on nickel or could form a hydroxide bridge with nickel. This phenomenon is not uncommon (32). Repulsion of charges appears not to be important because of the stability of $Cu_2(OH)_2^{+2}$ and other similar species such as $Cr_2(OH)_2^{+4}$, $Fe_2(OH)_2^{+4}$ and $Co_2(OH)_2^{+4}$ (23). Thus, an added degree of stability can be imparted to intermediates preceding the rate determining step. Further, this phenomenon is not unlike the Internal Conjugate Base Mechanism (ICB) which appears to impart added stability during formation reactions (33). These systems thus far have involved weak bases, yet have shown gains of 10 and 20 in reaction rate (19). Also, the presence of aromatic nitrogens in the nickel coordination sphere enhances the ICB effect (34). The present system involves a strong base, hydroxide, and does have an aromatic nitrogen in the coordination sphere. Analogous metal exchange systems involving copper as the attacking nucleophile also show enhanced rates due to $CuOH^{+}$. Table 14 lists the values. In all cases, not involving aroma-

TABLE 14

COMPARISON OF RATE CONSTANTS FOR THE ATTACK OF Cu^{+2} AND $CuOH^{+}$ ON VARIOUS COMPLEXES.

All rate constants in $\underline{M}^{-1}sec^{-1}$ at 25° C and μ = 0.1 $\underline{M}$

Complex	$k^{NiL}_{Cu^{+2}}$	$k^{NiL}_{CuOH^{+}}$ [a]	$\frac{k^{NiL}_{CuOH^{+}}}{k^{NiL}_{Cu^{+2}}}$	Ref.
$NiBPEDA^{+2}$	4.9×10^{-4}	.1080	220	This work
$Ni(trien)^{+2}$	2.7	80	30	11
$NiEDTA^{-2}$	.075	1.4[b]	18	9
$ZnEDTA^{-2}$	67	220	33	9

[a] Values of $k^{NiL}_{CuOH^{+}}$ have been calculated assuming $B_{11} = 5 \times 10^{-8}$.

[b] The data used to resolve $k^{NiEDTA^{-2}}_{Cu^{+2}}$ were not corrected for any hydrolyzed copper species.

tic nitrogens bonded to nickel, it can be seen that $CuOH^{+}$ is about 30 times more reactive than Cu^{+2}. The added factor of 7 between these complexes and $NiBPEDA^{+2}$ can be attributed to the presence of an aromatic nitrogen in BPEDA since, as previously mentioned, aromatic nitrogens increase the ICB effect.

The reactions involving $NiEDTA^{-2}$, $Ni(trien)^{+2}$ and $NiBPEDA^{+2}$ all have nickel nitrogen bond rupture as rate determining while the ZnEDTA system involves copper ligand bond formation as rate determining. Of the three possible explanations for the increased activity due to $CuOH^{+}$, the first, an increase in the stability of the dinuclear intermediate, can not explain why $CuOH^{+}$ reacts at an accelerated rate with ZnEDTA because the dinuclear intermediate forms after the rate determining step. The second explanation, a transition state, could explain all four systems but is based on the tenuous grounds of an acceleration in copper water loss due to hydroxide. The third possibility however, fits all four cases since a hydrogen bonded or hydroxide bridged intermediate would affect the value of K_{os}, the outer sphere association constant, to the same extent that it would affect the stability of a dinuclear intermediate. Therefore it is suggested that this is the most likely explanation for the increased reactivity of $CuOH^{+}$.

APPENDIX

An equation relating the concentration of $NiBPEDA^{+2}$ to the absorbance of a reaction solution was derived in the following manner.

The total absorbance is equal to the sum of the absorbances of the individual species as expressed in equation 1.

$$A_{total} = A_{CuL} + A_{NiL} + A_{Cu} + A_{Ni}$$

$$= b(\epsilon_{CuL}[CuL] + \epsilon_{NiL}[NiL] + \epsilon_{Ni}[Ni^{+2}] + \epsilon_{Cu}[Cu^{+2}] \quad (1)$$

The concentrations of Ni^{+2}, Cu^{+2} and $CuBPEDA^{+2}$ at anytime are related to the final concentrations and the concentration of $NiBPEDA^{+2}$.

$$[Cu^{+2}] = [Cu^{+2}]_f + [NiL] \quad (2)$$

$$[Ni^{+2}] = [Ni^{+2}]_f - [NiL] \quad (3)$$

$$[CuL^{+2}] = [CuL^{+2}]_f - [NiL] \quad (4)$$

Substituting equations 2, 3 and 4 into equation 1, gives

$$A_t = (\epsilon_{CuL}[CuL]_f + \epsilon_{Ni}[Ni^{+2}]_f + \epsilon_{Cu}[Cu^{+2}]_f$$

$$-\epsilon_{CuL}[NiL] + \epsilon_{Ni}[NiL] - \epsilon_{NiL}[NiL] + \epsilon_{Cu}[NiL])\,b \quad (5)$$

At equilibrium the absorbance due to $NiBPEDA^{+2}$ is negligible and

$$A_\infty = (\epsilon_{CuL}[CuL]_f + \epsilon_{Ni}[Ni^{+2}]_f + \epsilon_{Cu}[Cu^{+2}]_f)\,b \quad (6)$$

Substituting equation 6 into equation 5 and solving for the concentration of $NiBPEDA^{+2}$ gives the desired relation

$$[NiL] = \frac{A_t - A\infty}{(=\varepsilon_{CuL} + \varepsilon_{NiL} - \varepsilon_{Ni} + \varepsilon_{Cu})\,b} \qquad (7)$$

The constants appearing in Table 9 are defined in the following manner.

Stability constants

$$K_{NiL}^{Ni,H_nL} = \frac{[NiL^{+2}][H^+]^n}{[Ni^{+2}][H_nL^{+n}]} \qquad (8)$$

Proton association constants

$$K_{H_nL} = \frac{[H_nL^{+n}]}{[H^+][H_{n-1}L^{+(n-1)}]} \qquad (9)$$

BIBLIOGRAPHY

1. T. J. Bydalek and D. W. Margerum, J. Am. Chem. Soc., 83, 4326 (1961).

2. D. W. Margerum and T. J. Bydalek, Inorg. Chem., 1, 852 (1962).

3. T. J. Bydalek and D. W. Margerum, Inorg. Chem., 2, 678 (1963).

4. D. W. Margerum, Record Chem. Prog., 24, 237 (1963).

5. D. W. Margerum and T. J. Bydalek, Inorg. Chem., 2, 683 (1963).

6. T. J. Bydalek and M. L. Bloomster, Inorg. Chem., 3, 667 (1964).

7. D. W. Margerum, D. L. Janes and H. M. Rosen, J. Am. Chem. Soc., 87, 4463 (1965).

8. R. K. Steinhaus and R. L. Swann, in press.

9. D. W. Margerum, B. A. Zabin and D. L. Janes, Inorg. Chem., 5, 250 (1966).

10. J. J. Latterall, M. S. Thesis Purdue University, 1962.

11. P. J. Menardi, Doctoral Dissertation, Purdue University, 1966.

12. F. J. Welcher, The Analytical Uses of Ethylenediammine Tetraacetic Acid, p. 217, D. Van Nostrand Co., Princeton, N. J., 1958

13. D. H. Busch and J. C. Bailar, J. Am. Chem. Soc., 78, 1137 (1956).

14. D. W. Gruenwedel, Inorg. Chem., 7, 495 (1968).

15. J. D. Barger, R. D. Zachariasen and J. K. Romary, J. Inorg. Nucl. Chem., 31, 1019 (1969).

16. J. Bjerrum, Metal Ammine Formation in Aqueous Solution, P. Hasse and Son, Copenhagen, 1941.

17. H. B. Jonassen, R. B. LeBlanc and R. M. Rogan, J. Am. Chem. Soc., 72, 4968 (1950).

18. R. K. Steinhaus and Z. Amjad, Inorg. Chem., 12, 151 (1973).

19. D. B. Rorabacher and D. W. Margerum, Inorg. Chem., 3, 382 (1964).

20. H. Ohtaki and T. Kawai, Bull. Chem. Soc. Japan, 45, 1735 (1972).

21. D. D. Perrin, J. Chem. Soc., 3189 (1960).

22. K. J. Pedersen, Kgl. Danske Videnskab. Selskag, 20, 1 (1939).

23. M. Eigen and L. DeMaeyer, Technique of Organic Chemistry, A. Weissberger, Ed., Vol. VIII, Part II, 2nd Ed., Interscience Publishers, New York, 1963, pp. 1042, 1047.

24. L. G. Sillen and A. E. Martel, Stability Constants of Metal Ion Complexes, The Chemical Society, London, 1964.

25. G. A. Melson and R. G. Wilkens, J. Chem. Soc., 2662 (1963).

26. H. B. Jonassen, R. E. Reeves and L. Sogal, J. Am. Chem. Soc., 77, 2748 (1955).

27. R. L. Gustafson and A. E. Martel, J. Am. Chem. Soc., 81, 525 (1959).

28. J. E. Prue and G. Schwarzenbach, Helv. Chim. Acta, 33, 985 (1950).

29. R. C. Courtney, R. L. Gustafson, S. Chaberck and A. E. Martel, J. Am. Chem. Soc., 81, 519 (1959).

30. T. J. Swift and R. E. Connick, J. Chem. Phys., 37, 307 (1962).

31. R. K. Steinhaus and D. W. Margerum, J. Am. Chem. Soc., 88 441 (1966).

32. F. A. Cotton and G. Wilkinson, Advanced Inorganic Chemistry, 2nd Ed., pp. 796-908, Interscience Publishers, New York, 1966.

33. D. B. Rorabacher, Inorg. Chem., 5, 1891.

34. R. K. Steinhaus and J. A. Boersma, Inorg. Chem., 11, 1505 (1972).